Journal of Hydrology 531 (2015) 389–407

Contents lists available at ScienceDirect

Journal of Hydrology

journal homepage: www.elsevier.com/locate/jhydrol

Impact of spatial and temporal resolution of rainfall inputs on urban hydrodynamic modelling outputs: A multi-catchment investigation

Susana Ochoa-Rodriguez [a,*], Li-Pen Wang [b], Auguste Gires [c], Rui Daniel Pina [a], Ricardo Reinoso-Rondinel [d], Guendalina Bruni [e], Abdellah Ichiba [c,f], Santiago Gaitan [e], Elena Cristiano [e], Johan van Assel [g], Stefan Kroll [g], Damian Murlà-Tuyls [b], Bruno Tisserand [h], Daniel Schertzer [c], Ioulia Tchiguirinskaia [c], Christian Onof [a], Patrick Willems [b], Marie-Claire ten Veldhuis [e]

[a] Urban Water Research Group, Department of Civil and Environmental Engineering, Imperial College London, Skempton Building, London SW7 2AZ, UK
[b] Hydraulics Laboratory, KU Leuven, 3001 Heverlee (Leuven), Belgium
[c] Université Paris-Est, École des Ponts ParisTech, LEESU, 6-8 Av Blaise Pascal Cité Descartes, Marne-la-Vallée, 77455 Cx2, France
[d] Department of Geoscience and Remote Sensing, Faculty of Civil Engineering and Geosciences, Delft University of Technology, PO Box 5048, 2600 GA Delft, The Netherlands
[e] Department of Water Management, Faculty of Civil Engineering and Geosciences, Delft University of Technology, PO Box 5048, 2600 GA Delft, The Netherlands
[f] Conseil Général du Val-de-Marne, Direction des Services de l'Environnement et de l'Assainissement (DSEA), Bonneuil-sur-Marne, 94381, France
[g] Aquafin NV, Dijkstraat 8, 2630 Aartselaar, Belgium
[h] Veolia Environment Research and Innovation, Chemin de la Digue, BP 76, 78603 Maisons Laffitte Cedex, France

ARTICLE INFO

Article history:
Available online 27 May 2015

Keywords:
Urban hydrology
Spatial–temporal resolution
Radar rainfall
X-band radar
Urban drainage
Hydrodynamic models

SUMMARY

Urban catchments are typically characterised by high spatial variability and fast runoff processes resulting in short response times. Hydrological analysis of such catchments requires high resolution precipitation and catchment information to properly represent catchment response. This study investigated the impact of rainfall input resolution on the outputs of detailed hydrodynamic models of seven urban catchments in North-West Europe. The aim was to identify critical rainfall resolutions for urban catchments to properly characterise catchment response. Nine storm events measured by a dual-polarimetric X-band weather radar, located in the Cabauw Experimental Site for Atmospheric Research (CESAR) of the Netherlands, were selected for analysis. Based on the original radar estimates, at 100 m and 1 min resolutions, 15 different combinations of coarser spatial and temporal resolutions, up to 3000 m and 10 min, were generated. These estimates were then applied to the operational semi-distributed hydrodynamic models of the urban catchments, all of which have similar size (between 3 and 8 km^2), but different morphological, hydrological and hydraulic characteristics. When doing so, methodologies for standardising model outputs and making results comparable were implemented. Results were analysed in the light of storm and catchment characteristics. Three main features were observed in the results: (1) the impact of rainfall input resolution decreases rapidly as catchment drainage area increases; (2) in general, variations in temporal resolution of rainfall inputs affect hydrodynamic modelling results more strongly than variations in spatial resolution; (3) there is a strong interaction between the spatial and temporal resolution of rainfall input estimates. Based upon these results, methods to quantify the impact of rainfall input resolution as a function of catchment size and spatial–temporal characteristics of storms are proposed and discussed.

© 2015 The Authors. Published by Elsevier B.V. This is an open access article under the CC BY-NC-ND license (http://creativecommons.org/licenses/by-nc-nd/4.0/).

1. Introduction

The impact of spatial–temporal variability of rainfall on catchment response and the sensitivity of hydrological models to the spatial–temporal resolution of rainfall inputs have been active topics of research over the last few decades (e.g. Singh, 1997; Berndtsson and Niemczynowicz, 1988; Lobligeois et al., 2014). Several studies have shown that the spatial–temporal variability of rainfall fields can translate into large variations in flows; as a result, it is necessary to account for this variability in order to

* Corresponding author. Tel.: +44 (0)20 7594 6018.
E-mail addresses: s.ochoa-rodriguez@imperial.ac.uk (S. Ochoa-Rodriguez), Lipen.Wang@bwk.kuleuven.be (L.-P. Wang), auguste.gires@leesu.enpc.fr (A. Gires), r.pina13@imperial.ac.uk (R.D. Pina), r.r.reinosorondinel@tudelft.nl (R. Reinoso-Rondinel), G.Bruni@tudelft.nl (G. Bruni), abdellah.ichiba@leesu.enpc.fr (A. Ichiba), S.Gaitan@tudelft.nl (S. Gaitan), E.Cristiano@tudelft.nl (E. Cristiano), johan.vanassel@aquafin.be (J. van Assel), stefan.kroll@aquafin.be (S. Kroll), Damian.MurlaTuyls@bwk.kuleuven.be (D. Murlà-Tuyls), bruno.tisserand@veoliaeau.fr (B. Tisserand), Daniel.Schertzer@enpc.fr (D. Schertzer), ioulia.tchiguirinskaia@enpc.fr (I. Tchiguirinskaia), c.onof@imperial.ac.uk (C. Onof), Patrick.Willems@bwk.kuleuven.be (P. Willems), j.a.e.tenveldhuis@tudelft.nl (M.-C. ten Veldhuis).

http://dx.doi.org/10.1016/j.jhydrol.2015.05.035
0022-1694/© 2015 The Authors. Published by Elsevier B.V.
This is an open access article under the CC BY-NC-ND license (http://creativecommons.org/licenses/by-nc-nd/4.0/).

properly characterise hydrological response (Tabios and Salas, 1985; Berndtsson and Niemczynowicz, 1988; Krajewski et al., 1991; Obled et al., 1994; Singh, 1997; Chaubey et al., 1999; Arnaud et al., 2002; Syed et al., 2003; Smith et al., 2004; Kavetski et al., 2006). This is particularly the case in small urban catchments, which are characterised by fast runoff processes and short response times, and are therefore very sensitive to the spatial and temporal variability of precipitation (this variability was found to be significant even at the small scales of urban catchments (Emmanuel et al., 2012; Gires et al., 2014b)). In order to well represent urban runoff processes, high resolution precipitation information is therefore needed (Schilling, 1991; Faurès et al., 1995; Shah et al., 1996; Aronica and Cannarozzo, 2000; Einfalt, 2005; Tetzlaff and Uhlenbrook, 2005; Segond et al., 2007; Vieux and Imgarten, 2012; Schellart et al., 2012). This need has been further fuelled by recent developments in, and increasing use of, higher-resolution urban hydrological models (e.g. Fewtrell et al., 2011; Giangola-Murzyn et al., 2012; Pina et al., 2014), which allow incorporation of detailed rainfall, surface and runoff information. With regards to rainfall monitoring, significant progress has been made over the last few decades, including widespread increase in the use of weather radar rainfall estimates, generally provided by national meteorological services at 1 km/5–10 min resolutions. Multiple studies have been conducted in recent years aimed at analysing urban hydrological/hydraulic model sensitivity to the spatial–temporal resolution of rainfall inputs and at establishing required rainfall input resolutions for urban hydrological applications. However, there is not as yet a consensus on these topics.

A theoretical study undertaken by Schilling (1991) suggested that, for urban drainage modelling, rainfall data of at least 1–5 min and 1 km resolutions should be used. Another study undertaken by Fabry et al. (1994) suggested that finer resolution data (i.e. 1–5 min in time and 100–500 m in space) are required for urban hydrological applications. This however may vary according to the application (Einfalt et al., 2004; Einfalt, 2005); for detailed sewer system simulation, for example, it is believed that the spatial–temporal resolutions suggested in Fabry et al. (1994) are essential.

Berne et al. (2004) analysed the relation between catchment size and minimum required spatial and temporal resolutions or rainfall measurements in a study involving very high resolution precipitation data (~7.5 m/4 s) and runoff records from six urban catchments on the French Mediterranean coast (but not models were used). Their study suggests that for small urban catchments, of the order of 3 ha, ~1.5 km/1 min resolution, rainfall estimates are recommended, whereas for larger catchments, of the order of 500 ha, ~3 km/5 min estimates may suffice. Slightly more stringent resolution requirements were identified by Notaro et al. (2013): using high spatial–temporal resolution rain gauge records as input to the semi-distributed urban drainage model of a 700 ha urban catchment in Italy, the authors investigated the uncertainty in runoff estimates resulting from coarser resolution rainfall inputs and concluded that temporal resolutions below 5 min and spatial resolutions of ~1.7 km are generally required for urban hydrological applications.

Using a semi-distributed urban drainage model of a small urban catchment in London, and stochastically-downscaled rainfall estimates, Gires et al. (2012) and Wang et al. (2012) showed that the unmeasured small-scale rainfall variability, i.e. occurring below the typically available resolutions of 1 km in space and 5 min in time, may have a significant impact on simulated flows, with the impact decreasing as the drainage area of interest increases. A similar study was undertaken by Gires et al. (2014a), but this time using a fully-distributed model of a small catchment in Paris; similar results were obtained, but the fully-distributed model displayed higher sensitivity to the resolution of rainfall inputs.

More recently, Bruni et al. (2015) analysed the relationship between spatial and temporal resolution of rainfall input, storm and catchment scales, urban hydrodynamic model properties and modelling outputs. This was done using high resolution (100 m/1 min) rainfall data provided by polarimetric weather radar and a semi-distributed urban drainage model of a subcatchment in Rotterdam, the Netherlands. They showed that for a densely built, highly impervious urban catchment, modelling outputs are sensitive to high resolution rainfall variability and that deviations in model outputs significantly increase as rainfall inputs are aggregated to coarser scales, particularly at very small drainage areas (<1 ha).

As can be seen, few studies have analysed measured spatial–temporal variability of rainfall at the 1 min and 100 m scales and those which have not always involved hydrological/hydraulic models and/or are limited to single catchment studies. Hence, evidence to prove the added value of higher resolution rainfall estimates and to provide an answer about actual resolution requirements for urban hydrological applications is still insufficient. With the purpose of providing additional evidence in this direction, the present study investigates the impact of rainfall input variability for a range of spatial and temporal resolutions on the hydrodynamic modelling outputs of seven urban catchments located in each of the partner countries of the European Interreg RainGain project (http://www.raingain.eu/) (i.e. UK, France, Netherlands and Belgium). Rainfall estimates of nine storm events were derived from a polarimetric X-band radar located in Cabauw (The Netherlands). The original radar estimates, at 100 m and 1 min resolutions, were aggregated to spatial resolutions of 500, 1000 and 3000 m, and were sampled at temporal resolutions of 1, 3, 5 and 10 min. These estimates were then applied to high-resolution semi-distributed hydrodynamic models of the seven urban catchments, all of which have similar size (between 3 and 8 km^2), but different morphological, land use and model structure characteristics. Within the catchments, outputs were analysed at different nodes along the main flow path to investigate the effect of drainage areas of different sizes. Methodologies for standardising rainfall inputs and hydrological outputs were implemented to make results comparable. The impact of varying spatial–temporal resolutions of rainfall input on hydrodynamic model outputs was analysed in the light of storm and catchment characteristics. Based upon these results, current research needs and future work are discussed.

The paper is organised as follows. In Section 2, the pilot catchments, hydrodynamic models and radar-rainfall datasets are introduced. Methodologies for selecting relevant spatial–temporal resolution combinations and characterising spatial–temporal characteristics of the nine storms events are explained in Section 3, as well as methodologies used for feeding the rainfall inputs into the hydrodynamic models of the pilot catchments and for extracting and analysing the hydrodynamic modelling results. Results are presented and discussed in Section 4, followed by conclusions and recommendations in Section 5.

2. Pilot catchments and datasets

2.1. Pilot urban catchments

Seven urban catchments, located in four North-West European countries, were adopted as pilot locations in this study. With the aim of facilitating inter-comparison of results, catchment areas of similar size (3–8 km^2) were selected for testing. The main characteristics of the selected pilot catchments are summarised in Table 1. Moreover, images of the boundaries and sewer layouts of all pilot catchment can be found in Fig. 1. More detailed

Table 1
Summary characteristics of selected pilot urban catchments.

	Cranbrook (UK)	Torquay Town Centre (UK)	Morée-Sausset (FR)	Sucy-en-Brie (FR)	Herent (BE)	Ghent (BE)	Kralingen (NL)
Catchment ID	1	2	3	4	5	6	7
Area (ha)	865	570	560	269	512	649	670
Catchment length and width (km)*	6.10/1.42	5.35/1.06	5.28/1.06	4.02/0.67	8.16/0.63	4.74/1.37	2.12/3.16
Catchment shape factor (−)**	0.23	0.20	0.20	0.17	0.08	0.29	1.49
Slope (m/m)***	0.0093	0.0262	0.0029	0.0062	0.0083	0.0001	0.0003
Main flow direction (°)	239	270	198	138	40	235	152
Type of drainage system	Mostly separate, branched	Mostly combined, branched	Mostly separate, branched	Separate, branched	Mostly combined, branched	Mostly combined, branched	Mostly combined, looped
Is flow mainly driven by gravity?	Yes	Yes	Yes	Yes	Yes	Yes	No
Control elements	3 storage lakes	3 storage tanks, 1 pumping station	2 storage tanks	1 storage basin, 1 pumping station	5 main CSO's with control	15 pumping stations	20 pumping stations
IMP (%)****	52%	26%	37%	34%	27%	41%	48%
Predominant land use*****	R&C	R&C	R&C	R&C	R	R	R&C
Population density (per/ha)	47	60	70	95	20	24	154

* Length = Length of longest flow path (through sewers) to catchment outfall; Width = Catchment Area/Catchment Length.
** Shape factor = Width/Length (this parameter is lower for elongated catchments).
*** Catchment slope = Difference in ground elevation between upstream most point and outlet/catchment length.
**** IMP: total proportion of impervious areas in relation to total catchment area.
***** Predominant land use: R = residential; C = commercial.

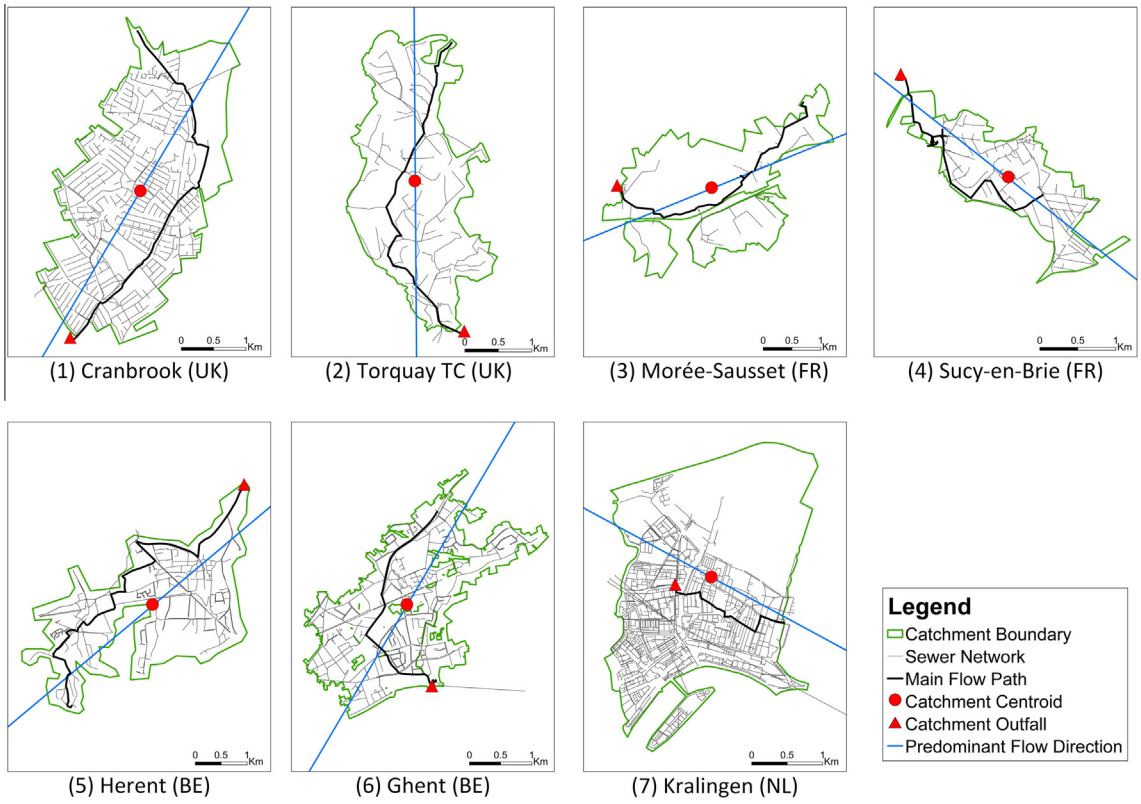

Fig. 1. Catchment boundary and sewer layout for the pilot urban catchments.

Table 2
Summary characteristics of the hydrodynamic models of the seven pilot catchments.

	Cranbrook, UK	Torquay Town Centre, UK	Morée-Sausset, FR	Sucy-en-Brie, FR	Herent, BE	Ghent, BE	Kralingen, NL
Total pipe length* (km)	98.05	41.29	15.30	4.02	67.42	83.44	142.65
Number of SC**	1765	492	47	9	683	1424	2435
Mean/Median/STD of SC size (ha)	0.49/0.37/0.71	1.16/0.93/1.09	11.92/8.00/10.34	29.89/13.07/27.47	0.71/0.34/1.27	0.46/0.23/0.89	0.12/0.09/0.13
Mean/Median/STD of SC slopes (m/m)	0.0560/0.0540/0.0334	0.0670/0.0470/0.0973	0.0056/0.005/0.0037	0.017/0.00575/0.0298	0.0221/0.0100/0.0282	0.0349/0.002/0.0459	0.0513/0.00812/0.0283
Mean/Median/STD of pipe slopes (m/m)	0.0103/0.0062/0.0138	0.0765/0.0488/0.1180	0.0062/0.0034/0.0141	0.0116/0.006/0.0145	0.0155/0.0073/0.0241	0.0030/0.00179/0.0078	0.0003/0.0000/0.0130
Rainfall-runoff volume estimation model	Fixed runoff coefficient for IMP/NewUK for PER	Wallingford model for IMP and PER	PER: Initial loss + runoff coefficient depending on rainfall depth and soil type. IMP: directly connected or not to the sewer network		Fixed runoff coefficient for all surfaces (0.8 for IMP; 0 for PER except some special ones)		Initial loss + fixed runoff coefficient for IMP; Horton's model for PER
Runoff routing model at SC	Double linear reservoir	Double linear reservoir	Single linear reservoir	Single linear reservoir	Double linear reservoir	Double linear reservoir	Runoff delay coefficient
Pipe flow routing model	Dynamic wave (full de St Venant Equations)						
Modelling software	InfoWorks CS 14	InfoWorks CS 14	Canoe 3.5	Canoe 3.5	InfoWorks CS 14	Infoworks CS 13	Sobek-Urban

* Pipe length is estimated based upon modelled pipes only.
** SC = sub-catchment.

information on each of these catchments can be found in the RainGain project website: http://www.raingain.eu/en/actualite/learn-more-about-ten-locations-where-raingain-solutions-will-be-implemented. As can be seen, the selected pilot catchments cover a wide range of morphological, topographic and land use conditions.

2.2. Urban drainage models of the pilot catchments

Verified and operational semi-distributed urban drainage models of each catchment were used in this study; their main characteristics are summarised in Table 2. In this type of models the whole catchment surface is split into sub-catchment units through which rainfall is applied. Each sub-catchment unit is treated as a lumped model within which rainfall is assumed to be uniform. Each sub-catchment comprises a mix of pervious (PER) and impervious (IMP) surfaces the runoff of which drains to a common outlet point, which corresponds to an inlet node of the sewer system (i.e. a gully or a manhole). Each sub-catchment is characterised by a number of parameters, including total area, length, slope and proportion of each land use, amongst others. Based upon these parameters, runoff volumes are estimated and routed at subcatchment scale using the rainfall–runoff and concentration models commonly employed in each country (see Table 2). Sub-catchment sizes of the models used in this study typically varied from 0.09 ha to 13.07 ha (median values). Sewer flows in all pilot catchment models are routed using the full de St. Venant equations (i.e. dynamic wave approximation).

2.3. High resolution precipitation data

High-resolution rainfall data were obtained by a dual-polarimetric X-band weather radar, IDRA hereafter, located in the CESAR observatory of the Netherlands (Figueras i Ventura, 2009; Leijnse et al., 2010). IDRA is a frequency modulated continuous wave (FMCW) radar working at 9.475 GHz. Its operational range is of 15 km with a range resolution of 30 m, approximately. IDRA is fixed at a height of 213 m from ground level; it scans at a fixed elevation angle of 0.5°, and rotates the antenna over 360° every minute. The technical specifications of IDRA are summarised in Table 3.

The accuracy of radar measurements can be affected by multiple factors, including clutter contamination and signal attenuation. In order to ensure good quality of the final radar product, several correction procedures were implemented; these are summarised next.

Signals of ground and moving clutter were identified and removed, using an optimum filter based on polarimetric spectra (Unal, 2009). Moreover, random fluctuations were separated from weather signals using a threshold of 3 dB above noise level. In addition, areas with linear depolarisation ratio (L_{dr}) larger than −15 dB were removed to ensure only rain particles are processed. Because IDRA works at X-band frequencies, received signals can

Table 3
Specifications of dual-polarimetric X-band weather radar IDRA from which high resolution precipitation data were derived for this study.

Radar type	FMCW
Polarisation	Dual polarisation
Frequency	9.475 GHz
Range resolution	3–30 m
Min range	230 m
Max range	<122 km
Max unambiguous radial velocity	19 m/s
Temporal resolution	1 min
Beamwidth	1.8°
Elevation	0.5°

experience large attenuation and as a result radar measurements such as reflectivity (Z) can be underestimated. However, the specific differential phase (K_{dp}) is immune to attenuation and therefore K_{dp} was used to correct reflectivity from attenuation effects as long as the received signals were not totally extinct (Otto and Russchenberg, 2011). Areas with extinct signals are typically located behind regions with heavy precipitation. In the implemented processing routines extinct areas were flagged and excluded from further processing.

K_{dp} is also immune to radar calibration errors and hail contamination. This makes K_{dp} suitable for rainfall rate estimation. However, K_{dp} at X-band frequencies can be contaminated by the backscattering component of the differential phase, which can introduce bias. In addition, with the purpose of maintaining low K_{dp} variability, K_{dp} is typically obtained at spatial resolutions of the order of 2–3 km (Bringi and Chandrasekar, 2001), which can be few times larger than the radar range resolution. Nonetheless, the approach by Otto and Russchenberg (2011), adopted in the present study, addresses both issues. First, the effect of the backscattering component is filtered out by using a theoretical relationship between the backscattering and the differential reflectivity. Second, K_{dp} is obtained at radar spatial resolution by using the self-consistency principle (Scarchilli et al., 1996).

Given the above considerations, for the present study rainfall rate (R) is estimated using K_{dp} for areas with $Z > 30$ dBZ, otherwise the corrected reflectivity is used according to Otto and Russchenberg (2012):

$$R = 13K_{dp}^{0.75} \quad (1)$$

$$z = 243R^{1.24} \quad (2)$$

where R, K_{dp}, and z are given in mm h^{-1}, degrees km^{-1}, and mm^6 m^{-3}, respectively. Although these steps improve the estimation of rainfall rate, there remain issues such as insect echoes, melting-layer contamination, and multi-trip echoes. Each of these echoes has a familiar pattern which can be detected through visual inspection: insects are noticeable at short ranges, at which radar reflectivity is highly sensitive; melting-layer contamination leads to strong echoes in the form of a ring around the radar; and multi-trip echoes can be identified in the reflectivity field by lengthened and weak echo lines. The data used in the present study were visually inspected to ensure that the effect of contamination by undesired echoes was minimal.

Rainfall estimates from IDRA were initially available in polar coordinates at temporal and spatial resolutions of 1 min and 30 m by 1.8° (i.e. radar beamwidth), respectively. However, to facilitate handling of the data, it had to be converted from polar to Cartesian coordinates. In this work, data were initially mapped to a regular grid of 100 m by 100 m; this is therefore the finest spatial resolution used as input for the urban drainage models in the present study. From the available IDRA dataset, eight storm events recorded between 2011 and 2014 were selected for this study. The selected events correspond to the most intense events recorded during these years and can be considered characteristic of North-West Europe. Nonetheless, it is worth mentioning that, being a research radar, IDRA does not operate continuously; therefore, not all intense storm events which occurred between 2011 and 2014 were recorded by the radar and the selected events include a combination of high intensity as well as moderate and low intensity storms. For each storm event a square area of 36 km^2, which is large enough to circumscribe the eight pilot catchments (considering their different shapes), was clipped from the total area covered by the radar and was used as input for the models of the pilot catchments. The area for analysis was selected such that it comprised the main rainfall cell(s) observed within the radar domain. The dates and main statistics of the selected storm events within the clipped (6 km × 6 km) area are summarised in Table 4. It is important to note that during the storm event on 18/01/2011, strong storm cells were observed in different areas of the radar domain. Given the high intensities and depths associated with the different areas, it was deemed appropriate to select two different areas within the radar domain for analysis. Consequently, for this storm event two sub-events were selected for analysis (i.e. E1 and E2). Storm profiles, snapshot images during the time of peak areal intensity as well as images of the rainfall depth accumulations for each storm event within the clipped area are shown in Fig. 2.

3. Methodology

3.1. Selection of rainfall input resolutions for analysis

To study the impact of spatial–temporal resolution of rainfall inputs on hydrodynamic model outputs, sixteen combinations of spatial–temporal resolutions were selected. The highest resolution of 100 m in space and 1 min in time was used as reference. Additionally, 15 resolution combinations were adopted based on the following considerations (the rationale behind the selected resolution combinations, as well as the selected combinations, are summarised in Fig. 3):

– In the framework of the simplest space–time scaling model that relies on a scaling anisotropy coefficient H_t (Deidda, 2000; Gires et al., 2011): when the spatial scale of the data is changed by a ratio of λ_{xy}, the temporal scale should be changed by a factor of $\lambda_t = \lambda_{xy}^{1-H_t}$. By combining the scale invariance property of Navier–Stokes equations with Kolmogorov's (1962) formulation, and assuming that the properties established for the atmosphere remain valid for rainfall, it is possible to show that H_t is expected to be equal to 1/3 (Marsan et al., 1996). This means that when the spatial scale is multiplied by 3, the temporal scale should be multiplied by 2 (i.e. $3^{1-1/3} \approx 2.08$) (Biaou et al., 2005;

Table 4
Characteristics of selected storm events (estimated based upon 1 min/100 m resolution estimates for the clipped (6 km × 6 km) area). Time is in UTC.

Event ID	Date	Duration	Total depth (areal average/pixel min/pixel max) (mm)	Max intensity over 1 min (areal average/individual pixel) (mm/h)
E1	18/01/2011	05.10–08.00 h	31.48/17.89/45.82	31.67/1120.20
E2	18/01/2011	05.10–08.00 h	36.12/16.48/47.17	26.48/124.00
E3	28/06/2011	22.05–23.55 h	8.94/4.46/17.64	28.42/241.82
E4	18/06/2012	05.55–07.10 h	10.12/8.03/11.76	11.62/24.11
E5	29/10/2012	17.05–19.00 h	5.34/1.20/13.64	7.05/82.83
E6	02/12/2012	00.05–03.00 h	4.94/2.39/7.86	6.59/38.57
E7	23/06/2013	08.05–11.30 h	4.19/0.73/13.39	9.41/306.55
E8	09/05/2014	18.15–19.35 h	4.48/1.40/8.88	12.98/66.76
E9	11/05/2014	19.05–23.55 h	5.99/1.22/12.65	10.53/246.74

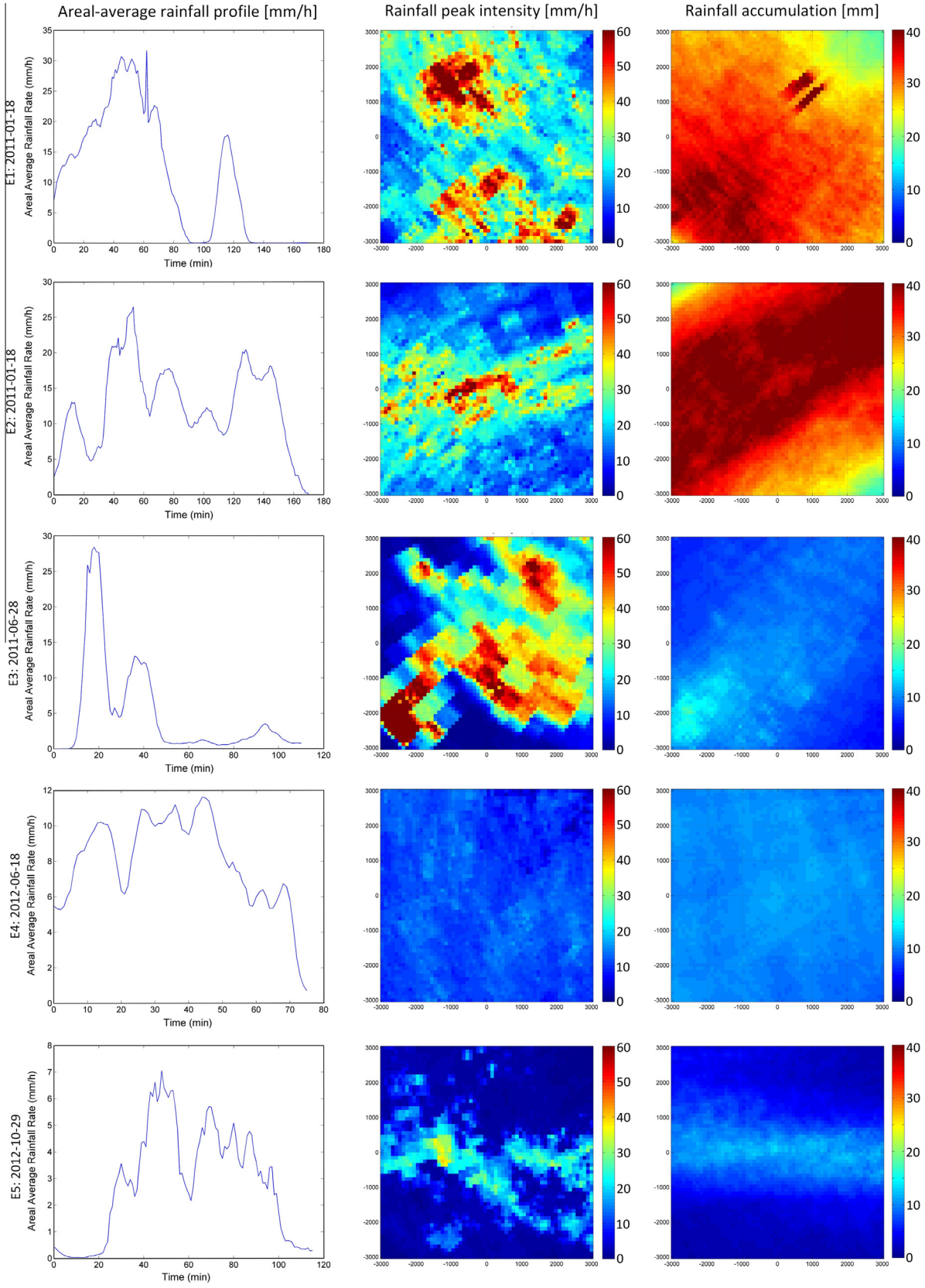

Fig. 2. Areal average storm intensity profile (left column), snapshot image during the peak intensity period of the storm (middle column) and total event accumulations for the storm events under consideration.

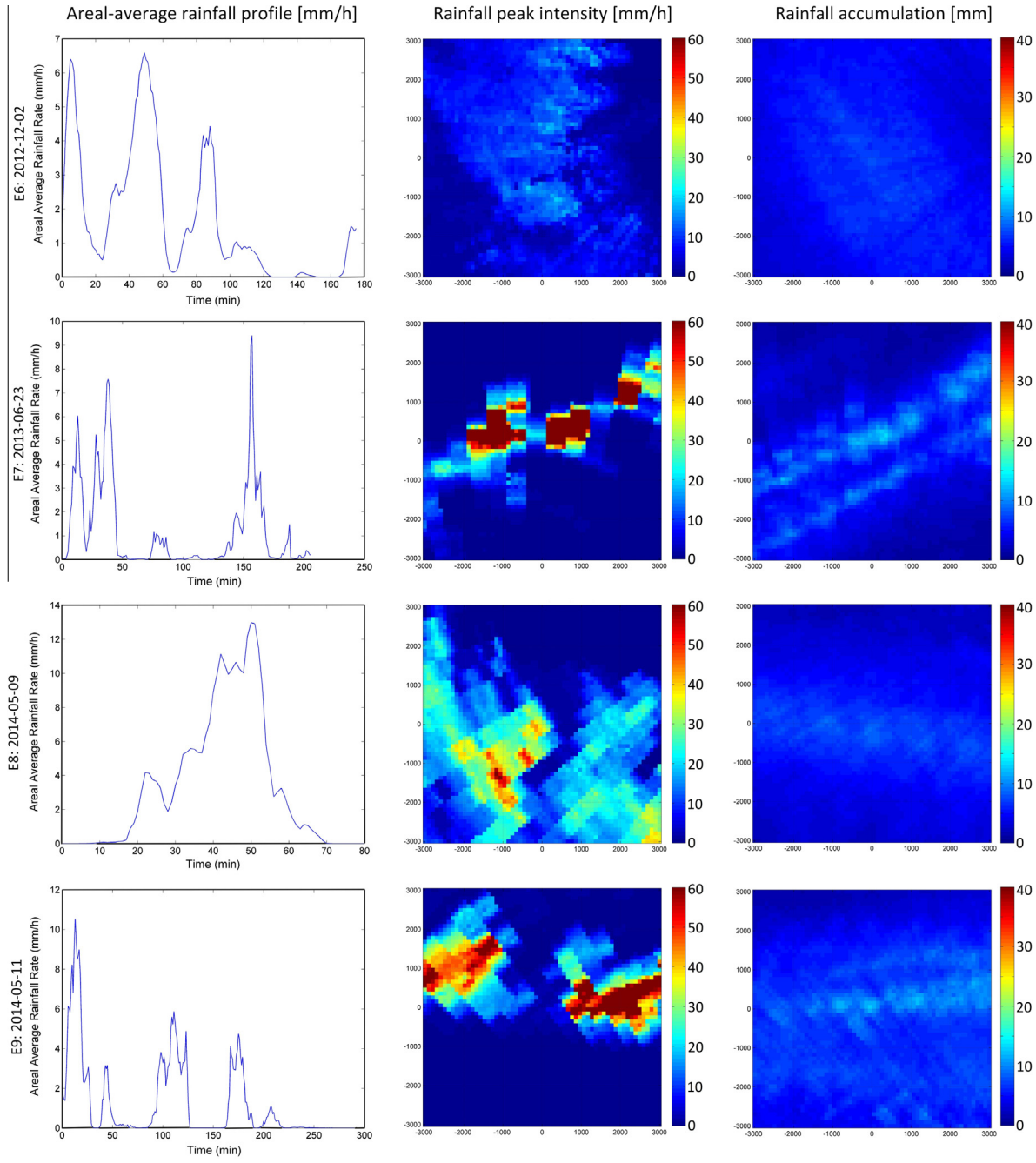

Fig. 2 (*continued*)

Gires et al., 2012). This leads to the following resolution combinations (indicated in blue in Fig. 3), upscaling from the reference resolution 100 m/1 min: 500 m/3 min; 1000 m/5 min; 3000 m/10 min.

- Operational resolutions: it is of interest to relate the results of this study to resolutions typically available from operational radar networks. The most common resolutions are 1000 m/5 min for national weather radar networks (e.g. in the UK, France, Netherlands, US). Other operational resolutions include: 1000 m/10 min (Malaysia), ~ 500 m/5 min (Belgium). Moreover, the equivalent resolutions of operational urban rain gauge networks are often of the order of several km in space and 1–15 min in time (WAPUG, 2002; Wang et al., 2013). The operational resolutions are indicated in yellow in Fig. 3.
- Berne et al. (2004) identified characteristic temporal and spatial scales relevant to describe the hydrological behaviour of urbanised catchments. They used a simple power law relationship to link lag time to the surface area of catchments. Based on this power law and on the characteristic spatial and temporal dimensions of storms typical of Mediterranean regions, the following approximate characteristic spatial–temporal resolutions were derived (indicated in green in Fig. 3): 1 min/1500 m (for catchment areas ~2.6 ha); 3 min/2600 m (for catchment areas ~100 ha); 5 min/3300 m (for catchment areas ~560 ha); 10 min/4700 m (for catchment area ~5600 ha).
- In addition to the resolution combinations mentioned in the literature based on atmospheric processes and catchment response characteristics, all remaining combinations of the

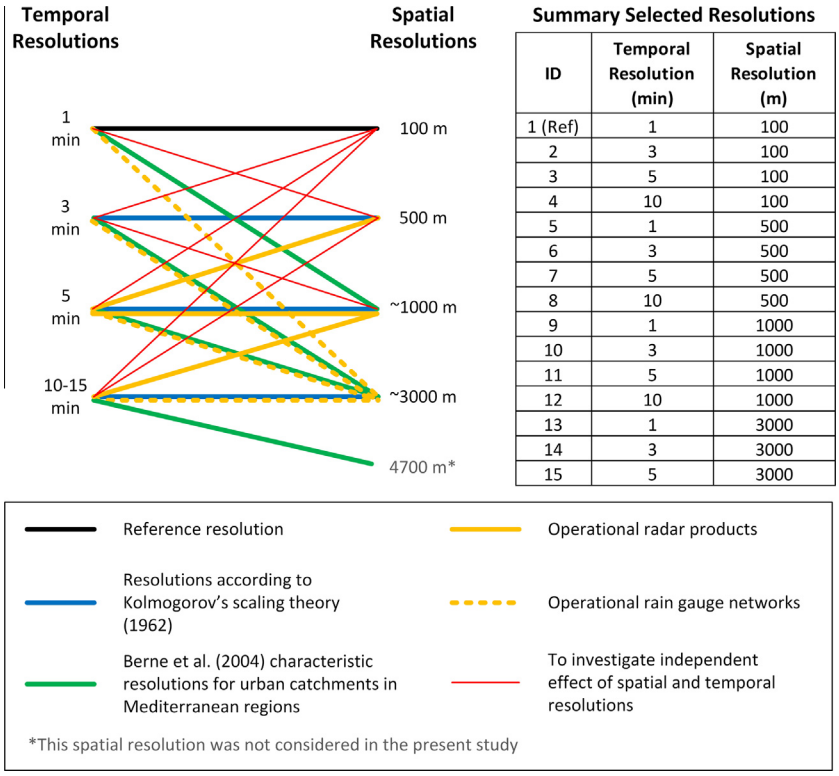

Summary Selected Resolutions

ID	Temporal Resolution (min)	Spatial Resolution (m)
1 (Ref)	1	100
2	3	100
3	5	100
4	10	100
5	1	500
6	3	500
7	5	500
8	10	500
9	1	1000
10	3	1000
11	5	1000
12	10	1000
13	1	3000
14	3	3000
15	5	3000

Fig. 3. Combinations of space and time resolutions of rainfall inputs investigated in this study. (For interpretation of the references to colour in this figure legend, the reader is referred to the web version of the article).

selected space and time scales were investigated, so as to enable the analysis of the 'marginal' as well as the combined effect of the different temporal and spatial resolutions (these are indicated in red in Fig. 3).

Using the finest resolution rainfall estimates (i.e. 100 m/1 min) as starting point, coarser spatial resolutions of up to 3000 m were generated through aggregation (i.e. averaging in space), and coarser temporal resolutions of up to 10 min were obtained by sampling a radar image at the desired time interval. The strategy to generate coarser temporal resolution estimates was chosen so as to replicate radar scanning strategies.

3.2. Spatial and temporal characterisation of storm events

Based upon the finest resolution rainfall data (i.e. 100 m/1 min), the following parameters were estimated which provide a measure of the spatial and temporal characteristics of the storm events under consideration. These parameters are used in Section 4 to analyse the observed impact of rainfall input resolution on hydrodynamic modelling results.

In the estimation of these parameters, only the (manually-selected) radar images over the peak period of the storm (i.e. period during which the core of the storm passes through the 6 km $\times$ 6 km clipped area) were considered. Including all radar images in the estimation would result in smooth parameters which do not reflect the dynamic and critical spatial–temporal features of the storm events, hence the analysis was conducted over the peak period only. It is worth noting that some of the storm events under consideration comprised more than one peak; when this was the case, each of the peaks was analysed separately and the peak with the most stringent characteristics and resolution requirements was adopted as representative of the storm event.

3.2.1. Spatial structure of storms and theoretically-required spatial resolution of rainfall inputs

A climatological variogram (Bastin et al., 1984; Berne et al., 2004; Bruni et al., 2015) was employed in this study to characterise the average spatial structure of rainfall fields over the peak storm period. Based upon the range of the variogram (r), which represents the limit of spatial dependence (Atkinson and Aplin, 2004), the integral range measure (A) (Lantuéjoul, 1991, 2002) was derived which can be considered as the mean area of the spatial structure captured by the radar images over the area of interest. Based upon A and following recommended signal/response requirements from communication theory (Shannon, 1948; Garrigues et al., 2006), a theoretically-required spatial resolution was estimated for each storm event under consideration.

The specific steps that were followed to obtain these parameters are the following:

(1) An empirical isotropic (semi-) variogram ($\gamma(h)$) was computed at each time step as:

$$\gamma(h) = \frac{1}{2n}\sum_{i}^{n}\left[(Z(\mathbf{x}) - Z(\mathbf{x}+h))^2\right] \quad (3)$$

where n is the number of all pairs of radar pixels separated by a distance h, Z are the rainfall rate values at the respective pixels and $\mathbf{x}$ corresponds to the centre of a given radar pixel.

(2) Each empirical variogram was normalised by dividing it by the sample variance.

(3) The normalised variograms obtained for each time step were averaged over the time period of analysis; this yields a climatological empirical variogram.

(4) An exponential variogram model was fitted to the empirical climatological variogram using weighted least square fitting (WLS). The exponential variogram function is the following:

$$\gamma(h) = C_0 + C\left[1 - \exp\left(-\frac{3\cdot|h|}{r}\right)\right] \quad (4)$$

where C_0 is the nugget, C is the sill, and r is the (practical) spatial range at which 95% of the sill is reached. It is worth noting that the two classical models that are used to fit climatological variograms are the exponential and spherical ones. For the storms under consideration both models were tested and a better fitting was generally obtained for the exponential one, hence it was adopted to describe the structure of the variogram.

(5) The integral range measure (A) was estimated as (Lantuéjoul, 1991, 2002):

$$A = \int_{h\in\mathcal{R}^2}\left(1 - \frac{\gamma(h)}{\sigma^2}\right)dh \quad (5)$$

where σ^2 is the variance and $\mathcal{R}^2$ is the 2-dimensional domain over which the variogram was derived. In simple terms, A corresponds to the area under the correlogram curve. For an exponential variogram model A is given by:

$$A = \frac{2\pi r^2}{9} \quad (6)$$

This measure summarises the (spatial) structural information of the variogram provided by the range and the fraction of total variance. As mentioned above, A can be considered as the mean area of the spatial structure captured by the radar images over the area of interest.

(6) The characteristic length scale of the storm event (r_c), which represents the mean extent of the spatial structure captured by the data (Garrigues et al., 2008), was estimated as the square root of A. For an exponential variogram model, r_c is given by:

$$r_c = \left(\frac{\sqrt{2\pi}}{3}\right)r \approx 0.836r \quad (7)$$

(7) In a study focusing on the quantification of the spatial heterogeneity of landscapes, Garrigues et al. (2006) demonstrated that by adopting a maximum pixel size equal to half of the characteristic length of the landscape image (i.e. $r_c/2$), it is possible to capture the major part of the spatial variability of land use. Their derivation followed Shannon's (1948) theorem, according to which the proper sampling frequency of a signal must be higher than twice the maximal frequency of this signal. Following Garrigues et al. (2006) approach, the coarsest spatial resolution (Δs_r) that is required to properly characterise a given storm event is therefore given by half of the characteristic length scale. For an exponential variogram:

$$\Delta s_r = \frac{r_c}{2} \approx 0.418r \quad (8)$$

In the case of a spherical variogram model, such as that used by Berne et al. (2004), $\Delta s_r = \frac{r_c}{2} \approx 0.396r$, where the ratio 0.396 is similar to the 1/3 ratio adopted by Berne et al. (2004), though it was derived with a different rationale.

3.2.2. Storm direction and velocity

Storm motion was estimated using the TREC (TRacking Radar Echoes by Correlation) method (Rinehart and Garvey, 1978), which is widely used in rainfall nowcasting (Tuttle and Foote, 1990; Laroche and Zawadzki, 1995; Horne, 2003; Li and Lai, 2004). This method analyses the cross-correlation of each two consecutive rainfall fields in order to derive a field of movement vectors (i.e. the displacements in easting and northing directions). Given that the study area was rather small (i.e. 6 km × 6 km), the domain was analysed as a whole (i.e. it was not divided into sub-domains, as is often done when large areas are analysed). A single movement vector representing the main velocity (both magnitude and direction) was thus obtained at each time step. The series of vectors obtained for the multiple time steps of the peak storm period were then averaged in order to obtain the mean velocity during this period (estimated velocity magnitudes are indicated in Table 5 of the results section).

Table 5
Estimated spatial and temporal characteristics and required rainfall input resolution for the storm events under consideration.

Event ID	Spatial range (r) (m)	Mean velocity ($\lvert\overline{v}\rvert$) (m/s)	Max. observable singularity (Small/Large)* (γ_s) (−)	Required spatial resolution (ΔS_r) (m)	Required temporal resolution (Δt_r) (min)
E1	4056.69	9.76	0.33/0.23	1694.77	5.79
E2	3524.76	9.91	0.33/0.23	1472.54	4.95
E3	4655.10	14.04	0.53/0.27	1944.77	4.62
E4	3218.91	11.71	0.62/0.37	1344.77	3.83
E5	2061.98	14.11	0.66/0.44	861.43	2.03
E6	3737.52	11.68	0.59/0.33	1561.43	4.46
E7	1702.93	13.95	0.92/0.50	711.43	1.70
E8	3644.43	18.40	0.55/0.24	1522.54	2.76
E9	2354.53	16.97	0.80/0.36	983.66	1.93

* γ_s values were estimated for two ranges of scales, for which scale invariance was found through multifractal analysis of rainfall images. These are: 100–600 m (small scales) and 600 m–6 km (large scales).

3.2.3. Theoretically-required temporal resolution of rainfall inputs

The coarsest temporal resolution (Δt_r) that is required to reflect the spatial structure of a storm as captured by data can be defined as the time needed to 'pass' the mean extent of the spatial structure (defined above). Based upon this definition, Δt_r can be computed as:

$$\Delta t_r = r_c/|\overline{v}| \quad (9)$$

where $|\overline{v}|$ is the magnitude of the mean velocity of the storm over the peak period.

3.2.4. Maximum observable singularity (γ_s)

While the geostatistical approach used to compute Δs_r provides a tangible estimate of the spatial features of a storm, it has the limitation of being a second-order approximation which means that it cannot properly reflect non-linear features (Schertzer and Lovejoy, 1987; Wang et al., 2015). With the purpose of further quantifying the spatial variability of rainfall fields, including higher-order statistical features, the concept of maximum observable singularity was used (Hubert et al., 1993; Douglas and Barros, 2003; Royer et al., 2008). This concept relies on the Universal Multifractal (UM) framework (see Schertzer and Lovejoy (2011) for a recent review) and quantifies the extremes one can expect to observe on a given sample of data according to its intrinsic variability. γ_s is estimated not at a single resolution, but across a range of resolutions over which scale invariance or scaling behaviour is detected (i.e. fluctuations at small scales are related to larger ones by the same scaling law). More precisely, a multifractal analysis is first conducted on the rainfall images for a given storm event, based upon which UM parameters are retrieved and scaling across different resolutions, as well as breaks in scaling, are identified. γ_s is subsequently computed from the UM parameters across the resolutions for which scale invariance is detected. By comparing γ_s over different scaling regimes, it is possible to detect changes in the spatial variability of rainfall fields as a result of resolution coarsening.

3.3. Application of rainfall inputs to models

Rainfall estimates at the selected temporal and spatial resolutions were applied as input to the hydraulic models of the seven urban catchments in such a way that the resulting modelling outputs were as comparable as possible. Firstly, rainfall estimates were applied such that the centroid of the clipped rainfall area (see Section 2.3) coincides with the centroid of each catchment (see Section 2.1). Moreover, rainfall inputs were applied in two relative directions: parallel and perpendicular to the main flow direction at each catchment. As explained in Section 3.2, storm direction was estimated based on the TREC method. The predominant flow direction at each pilot catchment was estimated based upon the slope of the linear regression of the (x, y) coordinates of the nodes located along the longest pipe flow path of each of the catchment models (Fig. 1). By applying rainfall inputs in the same relative direction to each catchment, variations in response due to differences in relative storm/flow direction (Singh, 1997) are avoided, thus making the results more comparable. Moreover, by applying rainfall inputs in these two relative directions it is possible to study variations in response due to differences in relative storm/flow direction.

3.4. Retrieval of hydraulic modelling results

For each of the hydraulic simulations carried out for each catchment (i.e. 9 storm events $\times$ 16 resolution combinations $\times$ 2 storm directions = 288), simulated flow time series at the downstream end of 8 pipes were retrieved for analysis. The 8 pipe locations were chosen such that the area that they drain (DA = drainage area) was approximately the following:

- 2 locations with DA $\sim$ 1 ha (i.e. characteristic length $(L = \sqrt{DA}) \sim 100$ m)
- 2 locations with DA $\sim$ 25 ha (i.e. $L \sim 500$ m)
- 1 locations with DA $\sim$ 100 ha (i.e. $L \sim 1000$ m)
- 1 locations with DA $\sim$ 300 ha (i.e. $L \sim 1700$ m)
- 1 locations with DA $\sim$ 500 ha (i.e. $L \sim 2200$ m)
- 1 locations with DA $\sim$ 600 ha (i.e. $L \sim 2500$ m)

These points for analysis were selected so as to assess the impact of rainfall input resolution in relation to the DA, which in previous studies has shown to play a dominant role in the requirements/impacts of rainfall input resolutions (e.g. Berne et al., 2004; Gires et al., 2012).

For the smallest catchments (e.g. Sucy-en-Brie (FR)), locations with the largest DAs do not exist. In these cases, simulation results for fewer points were retrieved. Conversely, in the case of catchments with total area >600 ha, results at an additional point corresponding to the downstream end of the catchment were retrieved. It is important to mention that the looped nature of the Kralingen catchment and the fact that flows may change direction throughout a storm event make it difficult to determine and estimate the area drained by a given pipe. For this catchment drainage areas were determined following the approach proposed by Bruni et al. (2015).

3.5. Evaluation of hydraulic modelling results

Using the hydraulic simulation results associated to the finest resolution rainfall estimates (i.e. 100 m/1 min) as reference, the following statistics were computed to quantify the impact of rainfall input resolution on the outputs of the hydraulic models of the seven urban. In order to allow inter-comparison of results from different catchments, storm events and points of analysis, only dimensionless statistics, which characterise different aspects of the simulated hydrographs, were used in this study.

- **Relative error (RE) in peak flow**:

$$RE_{st} = (Qmax_{st} - Qmax_{ref})/Qmax_{ref} \quad (10)$$

where RE_{st} is the relative error in the flow peak ($Qmax_{st}$) corresponding to a rainfall input of spatial resolution s and temporal resolution t, in relation to the reference (100 m/1 min) flow peak, $Qmax_{ref}$. Positive RE values indicate overestimation by the peak flow associated to the rainfall input st (i.e. $Qmax_{st}$), and vice versa. The RE has the advantage of being a 'tangible' statistic which evaluates the performance of a critical parameter as is the peak flow. It is important to note that very large RE values can be obtained when low flows are evaluated, even if the absolute difference in peak flows is small. Hence RE values must be analysed with caution.

- **Coefficient of determination (R^2)** and **regression coefficient (β)** resulting from a simple linear regression analysis applied between each simulated flows time series (*Qst*, resulting from a rainfall input of spatial resolution s and temporal resolution t) and the reference flow time series (*Qref*, resulting from the 100 m/1 min rainfall input). These two statistics provide an indication of how well the reference flows *Qref* are replicated by the 'simulated' *Qst* flows, both in terms of pattern and accuracy. The R^2 measure ranges from 0 to 1 and describes how much of the 'observed' variability in the *Qref* time series is explained by the 'simulated' one (i.e. *Qst*). In practical terms, R^2 provides a measurement of the similarity between the patterns of the reference flow time series (*Qref*) and the 'simulated' (*Qst*) flow time series. However, biases in modelled estimates cannot be detected from this measure (Murphy, 1988; Krause et al., 2005; Gupta et al., 2009). The regression coefficient, β, is therefore employed to provide this supplementary information to the R^2. $\beta \approx 1$ represents good agreement in the magnitude of *Qref* and *Qst* time series; $\beta > 1$ means that the simulated flows (*Qst*) are higher in the mean (by a factor of β) than the reference flows (*Qref*); and $\beta < 1$ means the opposite (i.e. *Qst* are lower in the mean than *Qref*). The R^2 and β statistics have the advantage of taking into account the entire time series (as opposed to RE, which only provides an assessment of Qmax), as well as of being relatively insensitive to the magnitudes of the flows under consideration.

4. Results and discussion

4.1. Spatial/temporal characteristics of storm events

The estimated spatial and temporal characteristics of the storm events, as defined in Section 3.2, are summarised in Table 5. As can be seen, the mean velocity of the nine storms analysed in this study varies from 9.8 m/s to 18.4 m/s. The combination of storm velocity and catchment dimensions (namely length and width) provides an indication of the time that it takes for a given storm cell to cross a catchment. Given that the length and width of the pilot catchments range between ~0.6 km and 8.2 km (see Table 1) and considering the minimum and maximum storm velocities, the time that it takes for the storms under consideration to cross the pilot catchments varies between ~0.6 min and 13.9 min.

With regards to the minimum required resolutions, it can be seen that the required temporal scales for all storm events are rather small and generally below the 5 min temporal resolution of rainfall estimates provided by most meteorological services based on national weather radar networks. Considering the fine requirements in terms of temporal resolution, significant changes in hydraulic performance would be expected when switching from

the finest temporal resolution of 1 min to coarser resolutions of 3, 5 and 10 min, which quickly exceed the minimum required temporal resolution for most storm events. In contrast, the required spatial resolutions are less stringent. In fact, the typical spatial resolution of rainfall estimates provided by national networks (i.e. 1000 m) matches the required spatial resolution for 6 out of the 9 storms under consideration. Given that all of the theoretically-required spatial resolutions are coarser than 500 m and most of them are coarser than 1000 m, little impact is to be expected in the hydraulic outputs associated to rainfall input resolutions of 500 m and 1000 m, as compared to those associated to the finest 100 m estimates. However, a drop in performance would be expected for hydraulic outputs corresponding to rainfall input resolutions of 3000 m, as this spatial resolution largely exceeds the theoretically-required resolution of all storm events.

Storm events 5, 7 and 9 have the 'finest' requirements, both in terms of temporal and spatial resolutions. Therefore, the impact of resolution coarsening for these three events is expected to be larger than for other events.

The scaling analysis prior to the computation of the maximum observable singularity (γ_s) suggests that the studied storms generally exhibit a scaling behaviour on two ranges of scales: 100–600 m (small scales) and 600 m–6 km (large scales). The actual location of the scaling break varies from approximately 400 m to 800 m, depending on the event. With the purpose of allowing inter-comparison of γ_s values, these are reported for the same ranges of scales for all storm events (i.e. 100–600 m and 600 m–6 km; see Table 5), Fig. 4 shows plots of the theoretically required spatial resolution (Δs_r) as a function of γ_s. Before proceeding to the analysis of these parameters, it is important to note that the limited range of scales available for the scaling analysis and computation of γ_s (due to the small domain of the X-band radar) means that results are not very robust and should be interpreted as trends. Nevertheless, they provide useful and complementary insights into the intrinsic variability of the rainfall fields under consideration. The first interesting finding of this analysis is the identification of two different scaling regimes, which highlights the importance of measuring rainfall at high resolution (i.e. below the identified scaling break) in order to properly capture extremes, which cannot be extrapolated from coarser scale measurements. Secondly, from Fig. 4 it can be seen that, for both scaling regimes, the theoretically required spatial resolution (Δs_r) decreases with increasing γ_s. This means that data at higher spatial resolution are required to well characterise storms which display higher intrinsic variability. This is logical and indicates that the outputs of the two analysis approaches used in the present study (i.e. geostatistical and multifractal) provide consistent results with regards to observed rainfall variability and extremes. However, it is worth noting that the required spatial resolutions (Δs_r) estimated with the geostatistical approach are mostly within the larger scale regime identified from the fractal analysis. This suggests that the geostatistical approach may be insufficient to characterise small scale, non-linear spatial features present in rainfall fields. This highlights the complementarity between the information provided by the two approaches, though more work is needed to better understand their relationship and optimise the way in which this information is used.

The way in which these spatial–temporal characteristics of rainfall relate to the impact of rainfall input resolution on hydrodynamic modelling results is investigated in the next section.

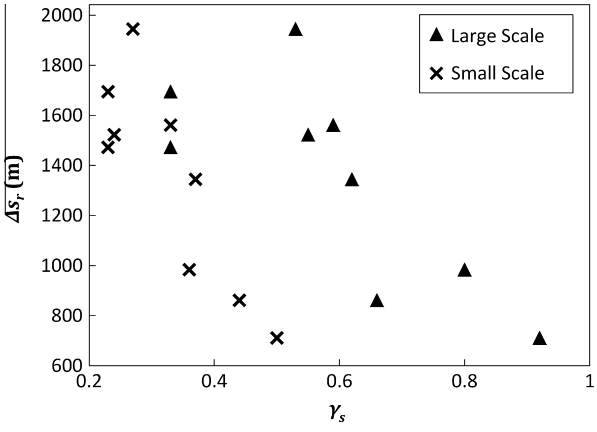

Fig. 4. Theoretically required spatial resolution (ΔS_r) as a function of maximum observable singularity (γ_s), for small (100–600 m) and large (600 m–6 km) scale ranges.

4.2. Hydrodynamic modelling results

Hydrodynamic modelling outputs are analysed based upon the dimensionless statistics introduced in Section 3.5: relative error in flow peaks (RE), coefficient of determination (R^2) and regression coefficient (β). In this section general trends observed in the hydraulic outputs are first identified. Afterwards, a detailed analysis is conducted to better understand the relationship between storm characteristics, catchment drainage area and the impact of rainfall input resolution on hydrodynamic modelling results.

4.2.1. General trends observed in hydrodynamic modelling results

In Fig. 5 performance statistics for all rainfall inputs are plotted as a function of drainage area (DA) size, for storms applied parallelly and perpendicularly to the catchments' main flow direction. At a glance and as was expected, a general trend can be identified of the impact of rainfall input resolution to decrease as drainage area increases. Moreover, the coarsening of temporal resolution generally appears to have a stronger influence as compared to the coarsening of spatial resolution; this is especially the case for small drainage areas. The stronger impact of temporal resolution over spatial resolution is in agreement with the estimated required temporal and spatial resolutions discussed in Section 4.1, as well as with previous studies (Krajewski et al., 1991; Meselhe et al., 2009; Notaro et al., 2013). The strong impact of temporal resolution coarsening can be partly explained by the way in which coarser temporal resolutions were obtained (i.e. by sampling radar images at the desired time resolution, in order to replicate radar scanning strategies); this is further discussed in Section 5.

In terms of magnitudes, as captured by RE and β statistics, a general underestimation tendency is observed as space and time resolutions of rainfall inputs become coarser (notice general trend of RE < 0 and β < 1). Noteworthy is the fact that coarser spatial resolutions systematically lead to underestimation of flows (notice behaviour of 3000 m resolutions denoted by red to yellow triangular markers), while coarser temporal resolutions have a more random effect and occasionally lead to large overestimation of flows. The underestimation associated with coarser spatial resolutions can be partly due to the smoothing of peak rainfall intensities which occurs when rainfall is averaged in space. In addition, it can also be explained by the fact that the cores of the storms were centred on the catchments; thus, as the spatial resolution of rainfall inputs approaches catchment size, storm water may be transferred outside of the catchment boundaries (Ogden and Julien, 1994; Bruni et al., 2015). The random effect of the coarsening of temporal resolution on flow magnitudes can in part be explained by the way in which the varying temporal resolutions were obtained (i.e. by sampling). It is interesting to note that, as DA increases, the random effect of temporal resolution on flow magnitudes decreases and a systematic underestimation tendency becomes clearer. In terms of R^2, it can be seen that the coarsening of

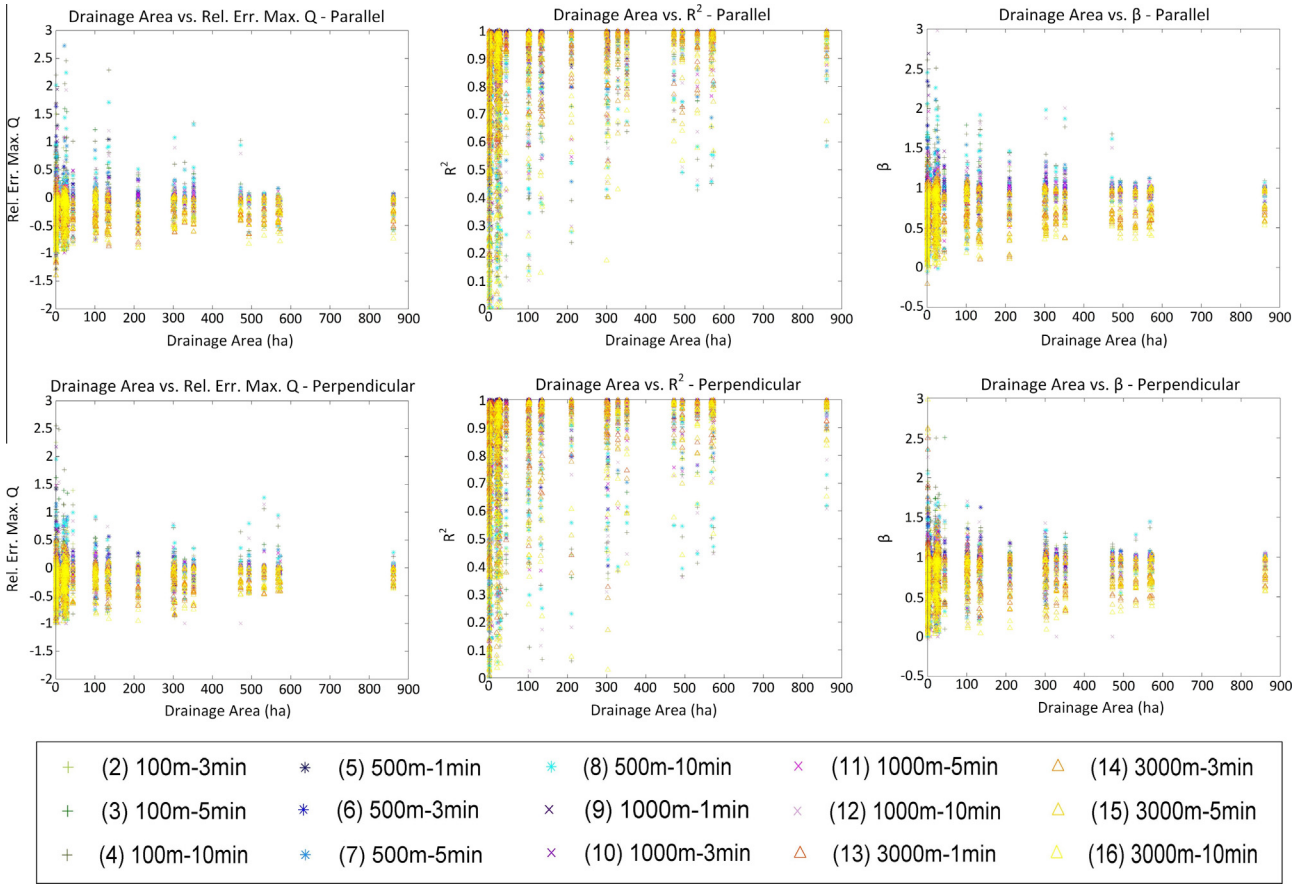

Fig. 5. Scatterplots of performance statistics relative error in maximum flow peak, R^2 and β versus drainage area sizes for 15 resolution combinations relative to the reference resolution of 1 min/100 m.

temporal resolution can easily alter the pattern of flow hydrographs: the lowest R^2 values are associated to the coarsest temporal resolutions, even when the associated spatial resolution is relative fine. Large drops in R^2 are also observed at spatial resolutions of 3000 m, which are significantly larger than the theoretically required spatial resolutions estimated for the storm events under consideration.

Regarding storm direction, similar trends are observed when storms are applied parallel and perpendicular to the predominant flow direction in the catchments (top and bottom plots in Fig. 5, respectively). Differences in response behaviour in relation to rainfall input resolutions for different storm direction would be expected particularly for elongated catchments. Such differences can be seen in some cases at the level of individual storms and catchments (plots not shown here), but these are rather small and do not have a significant impact on the general trends observed in summary statistics over all events and catchments. Given that a similar behaviour is observed for both relative storm directions, from now onwards only results for the parallel storm direction will be displayed and discussed. A detailed investigation of the impact of storm direction and individual catchment behaviour remains a topic for future study.

It is important to mention that some of the points of analysis at the different pilot catchments are subject to strong hydraulic controls (see Table 1). These controls influence flow behaviour and may lead to different sensitivity to rainfall input resolutions. To investigate this effect, the summary statistics shown in Fig. 5 were plotted separately for points with and without control elements. The resulting plots showed similar trends, indicating that control elements do not induce significantly different sensitivity to rainfall input resolution for the investigated storms, catchments and drainage area sizes.

Fig. 6 shows boxplots of the performance statistics by spatial–temporal resolution, per group of drainage area (DA) sizes. These boxplots allow direct comparison of the performance of different rainfall inputs. Moreover, the separation by DA sizes allows for a partial removal from the analysis of the impact of catchment parameters on hydraulic outputs. The following groups of DA sizes were defined, corresponding with the spatial resolutions investigated in this study:

- DA1: 0.7–1.3 ha (i.e. characteristic length ($L = \sqrt{DA}$) ~ 100 m)
- DA2: 20–30 ha ($L \sim 500$ m)
- DA3: 85–135 ha ($L \sim 1000$ m)
- DA4: 300–800 ha (1000 m < L < 3000 m)

From these boxplots it can clearly be seen that the temporal resolution of rainfall input has a bigger impact on simulated flows than spatial resolution, thus confirming the initial findings derived from Fig. 5 and from the analysis of spatial–temporal characteristics of storms (Section 4.1). The results show that coarse temporal resolutions of 5–10 min can lead to large errors, even if spatial resolution is high. This also affects hydrograph shape, as reflected by low R^2 values. In agreement with Fig. 5, it can be seen that sensitivity to rainfall input resolution decreases with drainage area size: drainage areas of spatial scales of 100–500 m show high sensitivity to temporal resolution coarsening and comparatively moderate sensitivity to spatial resolution coarsening. Drainage areas of spatial scale above 1000 m display lower sensitivity to space and time resolution. Large errors due to spatial resolution coarsening occur

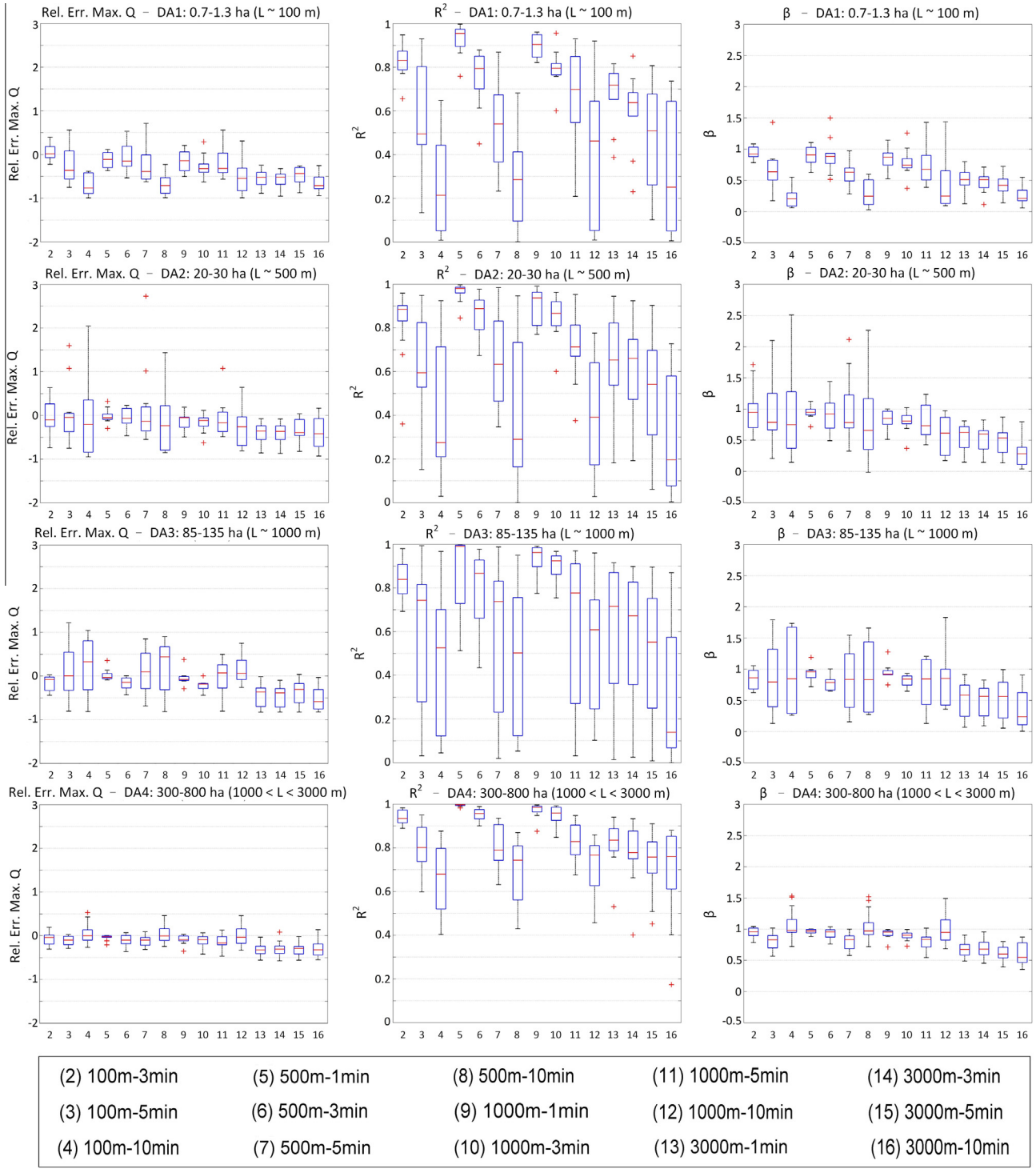

Fig. 6. Box plots of performance statistics relative error in maximum flow peak, R^2 and β per rainfall input resolution, per group of drainage area sizes. Note that the boxplots' whiskers extend 1.5 times the interquartile range below the first quartile (Q1) and above the third quartile (Q3), respectively. Points beyond this distance are represented as outliers.

at 3000 m resolution, for all drainage area sizes. The trends observed in Fig. 6 corroborate previous findings from Fig. 5 and provide confirmation that the theoretically-derived required spatial and temporal resolutions are sound.

An interesting feature that can be observed in Fig. 6 is the interaction and mutual dependence between temporal and spatial resolutions. Notice, for instance, that the 1000 m/5 min (one of the resolution combinations derived from Kolmogorov – see Fig. 3) associated outputs generally display a better performance than the 100 m/5 min ones, thus confirming the need for agreement between spatial and temporal resolution. The dependence between spatial and temporal resolutions has been widely discussed (e.g. Kolmogorov, 1962; Schertzer and Lovejoy, 1987; Marsan et al., 1996; Deidda, 2000; Gires et al., 2012), but there is

not as yet much evidence in urban hydrology to corroborate this hypothesis. The results of this study do provide evidence to support it.

The findings from Figs. 5 and 6 are generally in agreement with the findings and recommendations of Berne et al. (2004), but some differences are found. Berne et al. (2004) derived a relationship between space and time resolution of rainfall input required for urban hydrological analysis, based on catchment sizes of 10–10,000 ha in the Mediterranean region. The relationship they derived corresponds to a minimum rainfall resolution of 1 min/1.5 km for catchments smaller than 10 ha; 6 min/3.7 km for catchments of about 1000 ha. The temporal resolution they suggest for small drainage areas is in agreement with the findings of the present study; however, in relation to the spatial resolution, the present study suggests that for small drainage areas significant differences in flow estimates can be caused by changes in spatial resolution between 100 m, 500 m and 1000 m, at 1 min time resolution. In addition, the present study suggests that even for larger basins, relevant information is lost at time resolutions below 5 min.

4.2.2. Analysis of rainfall input resolution versus resolution requirements based on characteristic space–time scale of storm events

To investigate the impact of the spatial–temporal characteristics of storms on the observed variability in runoff estimates resulting from different rainfall input resolutions, performance statistics were plotted as a function of the following spatial and temporal scaling factors, as well as a function of a combined spatial–temporal factor which accounts for spatial–temporal scaling anisotropy (described in Section 3.1):

$$\theta_s = \left(\frac{\Delta S_r}{\Delta S}\right) \tag{11}$$

$$\theta_t = \left(\frac{\Delta t_r}{\Delta t}\right) \tag{12}$$

$$\theta_{st} = \left(\frac{\Delta S_r}{\Delta S}\right)\left(\frac{\Delta t_r}{\Delta t}\right)^{\frac{1}{1-H_t}} \tag{13}$$

where θ is a spatial–temporal scaling factor, ΔS_r and Δt_r are the required spatial and temporal resolutions estimated based upon storm characteristics (see Table 5), ΔS and Δt are the space and time resolutions of the rainfall inputs applied in model simulation and H_t is the scaling anisotropy factor, defined in Section 3.1, which theoretically has a value of 1/3.

Figs. 7 and 8 show performance statistics R^2 and β as a function of the scaling factor θ for scaling in space, scaling in time and combined spatial–temporal scaling, accounting for anisotropy. Relative errors (RE) plots were not included due to space constraints and given that these display a very similar behaviour to that of the β plots. Same as in Fig. 6, in Figs. 7 and 8 plots are displayed per group of drainage area (DA) sizes, in order to partially remove from the analysis the impact of catchment parameters on hydraulic outputs. In Figs. 7 and 8, for θ values above 1, the applied rainfall input resolution is finer than the theoretically required spatial–temporal resolution, estimated based upon storm characteristics (see Table 5). In the case of the spatial scaling factor (θ_s) alone (first row in Figs. 7 and 8), significant dispersion is observed in the plots and although performance statistics generally improve as θ_s increases, the improvement is not significant and the trend is rather unclear. In contrast, in the case of the temporal scaling factor (θ_t) (middle row in Figs. 7 and 8) a more clear pattern can be observed in the plots, with performance statistics visibly improving at larger values of θ_t. In the case of the combined factor (θ_{st}) (bottom row in Figs. 7 and 8) a significantly clearer pattern can be identified, with performance consistently improving for higher θ_{st} values, whereby small drainage areas remain more sensitive. While some dispersion can still be seen in the plots of combined factor (θ_{st}) vs. performance statistics, the fact that a significantly clearer pattern is observed in the θ_{st} plots, in comparison to the plots of the independent factors θ_s and θ_t, suggests that in order to properly represent the effect of temporal and spatial resolution

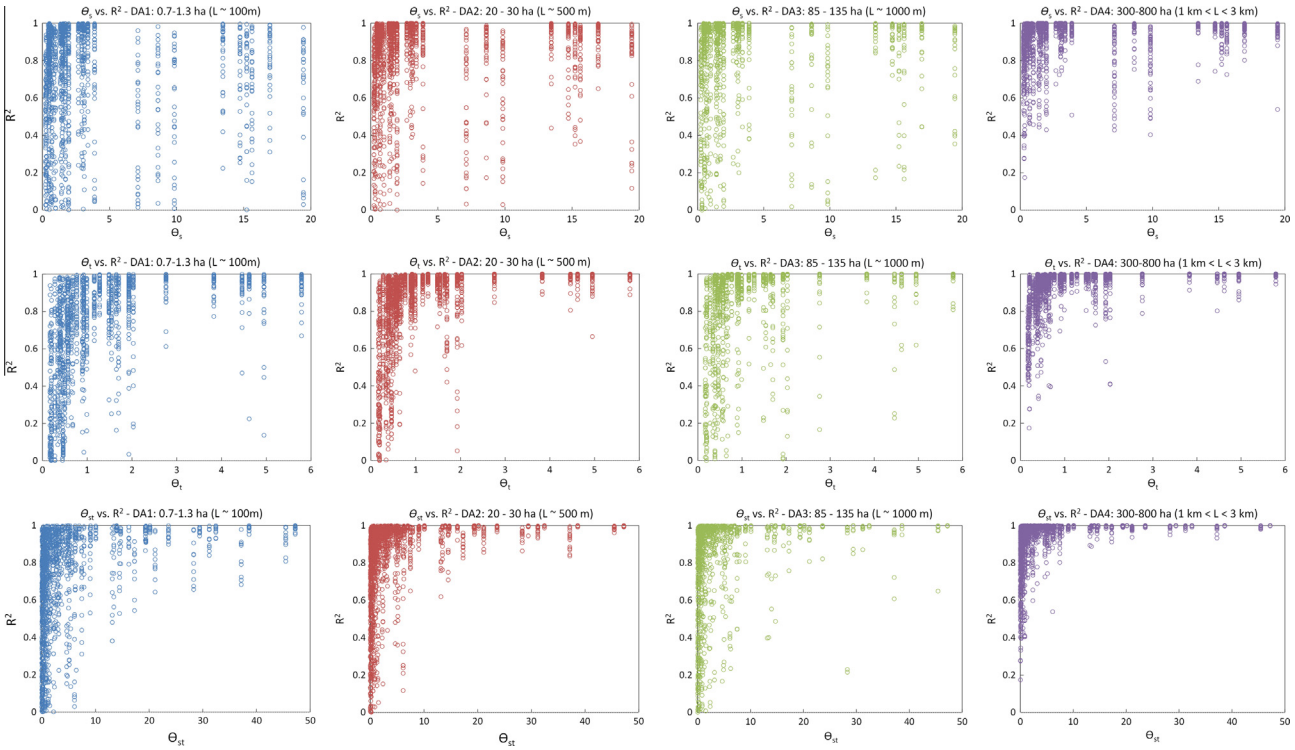

Fig. 7. Scatterplots of performance statistic R^2 as a function of scaling factors θ_s (top row), θ_t (middle row) and θ_{st} (bottom row), for 4 groups of drainage area sizes.

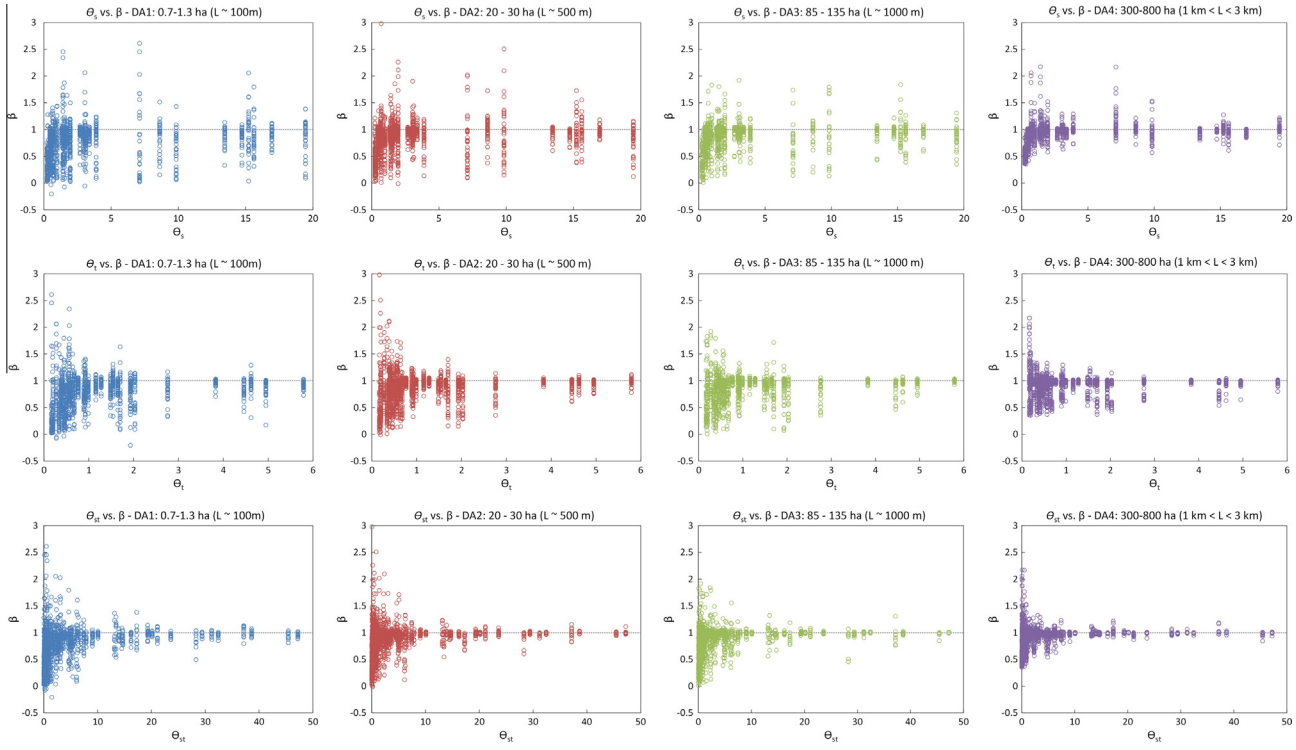

Fig. 8. Scatterplots of performance statistic β as a function of scaling factors θ_s (top row), θ_t (middle row) and θ_{st} (bottom row), for 4 groups of drainage area sizes.

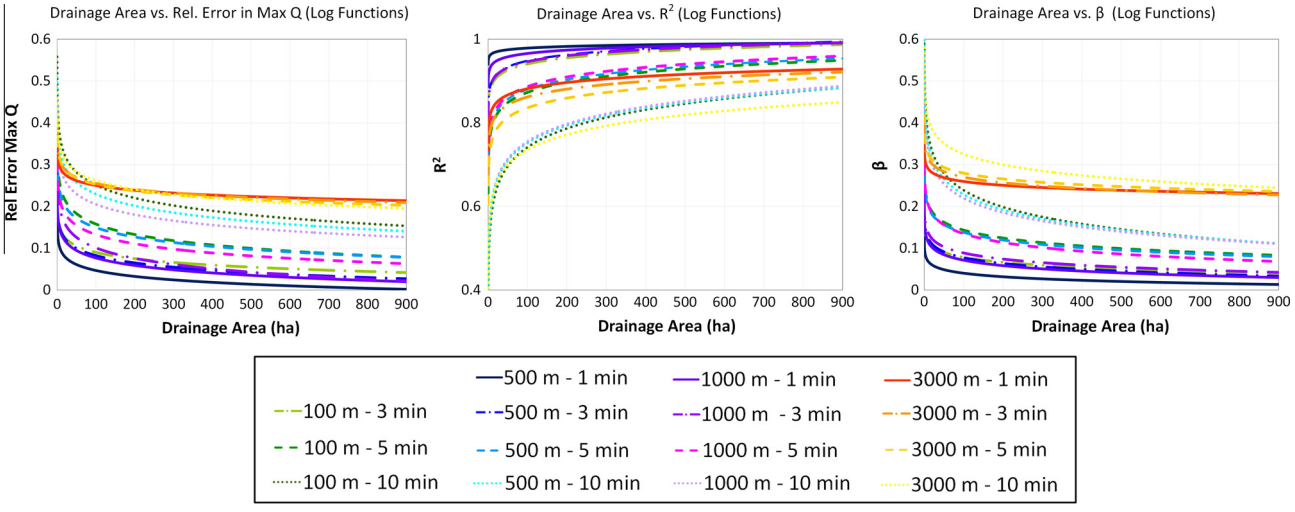

Fig. 9. Logarithmic functions fitted to data of performance statistics relative error in maximum flow peak, R^2 and β as a function of drainage area size, for different space–time resolution combinations. Line type denotes different temporal resolutions (1 min = solid; 3 min = dash-dot; 5 min = dashed; 10 min = dotted) and colour range denotes different spatial resolutions (100 m = green; 500 m = blue; 1000 m = purple; 3000 m = orange). (For interpretation of the references to colour in this figure legend, the reader is referred to the web version of this article).

of rainfall inputs, these must be considered together. This corroborates the interaction that exists between the two resolutions. Future work will focus on further investigating these interactions, along with other catchment and model factors which influence the results and may be responsible for the remaining dispersion observed in the θ_{st} plots.

4.2.3. Analysis of hydrodynamic response statistics in relation to rainfall input resolution and drainage area size

In Fig. 9, performance statistics were plotted as a function of drainage area size, for different spatial–temporal resolution combinations. A logarithmic function was fitted to the resulting plots using the least squares method. The function structure was defined as

$$Performance\ Stat = a \cdot \ln DA + b \tag{14}$$

The obtained a and b parameters and the associated mean square errors (MSE) of the fitting are summarised in Table 6.

The logarithmic functions provide a rough estimate of what hydrodynamic modelling performance can be expected for a given rainfall input resolution and catchment drainage area. For instance, for drainage area size of 100 ha, relative errors in maximum flow peak are expected to be below 0.1 for resolution combinations of 1 min/100–1000 m, while errors above 0.2 are expected for combinations of 10 min/100–1000 m and 1–10 min/3000 m resolution.

Based on the logarithmic functions plotted in Fig. 9, operational resolution of 5 min/1000 m provided by many national weather

Table 6
Parameters a and b and MSE-values for logarithmic function fitting, for performance statistics relative error (RE) in maximum flow peak, β and R^2.

Res ID	a Abs RE	b Abs RE	MSE Abs RE	a R^2	b R^2	MSE R^2	a Abs β	b Abs β	MSE Abs β
2	−0.0221	0.1920	0.0255	0.0211	0.8439	0.0143	−0.0172	0.1577	0.0181
3	−0.0361	0.3242	0.0694	0.0349	0.7120	0.0334	−0.0274	0.2696	0.0361
4	−0.0444	0.4557	0.2265	0.0648	0.4432	0.0605	−0.0583	0.5073	0.0812
5	−0.0205	0.1412	0.0182	0.0056	0.9528	0.0054	−0.0123	0.0969	0.0090
6	−0.0253	0.1988	0.0246	0.0208	0.8525	0.0093	−0.0201	0.1702	0.0163
7	−0.0325	0.2991	0.0802	0.0336	0.7254	0.0309	−0.0266	0.2605	0.0329
8	−0.0404	0.4158	0.1642	0.0604	0.4738	0.0605	−0.0534	0.4745	0.0675
9	−0.0259	0.1959	0.0276	0.0115	0.9130	0.0082	−0.0189	0.1585	0.0175
10	−0.0361	0.2674	0.1594	0.0207	0.8510	0.0111	−0.0211	0.1860	0.0172
11	−0.0317	0.2786	0.0598	0.0333	0.7334	0.0294	−0.0303	0.2744	0.0307
12	−0.0358	0.3698	0.1023	0.0603	0.4779	0.0616	−0.0498	0.4489	0.0610
13	−0.0166	0.3265	0.0539	0.0214	0.7832	0.0310	−0.0132	0.3207	0.0501
14	−0.0209	0.3512	0.0532	0.0271	0.7372	0.0386	−0.0194	0.3596	0.0530
15	−0.0227	0.3574	0.0793	0.0334	0.6821	0.0451	−0.0200	0.3719	0.0579
16	−0.0304	0.4021	0.0939	0.0517	0.4979	0.0699	−0.0368	0.4947	0.0676

radar networks is expected to result in relative errors in flow peak of about 0.2 for small drainage areas (1–10 ha) down to about 0.1 for drainage area sizes of up to 800 ha. R^2 and β values are expected to vary between 0.8 and 0.95 and between 0.3 and 0.7 for drainage area ranging from 1 to 800 ha.

While these results provide an indication of expected performance for varying rainfall input resolutions, they should be interpreted with caution. As values in Table 6 show, MSE-values are generally low for temporal resolutions of 1–3 min, but tend to decrease for lower temporal resolution and for spatial resolution above 1000 m.

Besides providing a practical estimate of the performance that can be expected for a given rainfall input resolution, the fitted logarithmic functions provide useful insights into the impact and interaction of spatial and temporal resolutions. In the case of relative error in peak flow and most evidently in the case of β, it can be seen that the fitted curves are grouped into four main sets: three of them corresponding to a given temporal resolution (and varying spatial resolutions from 100 m to 1000 m), and a fourth group corresponding to all the curves of spatial resolution 3000 m and varying temporal resolutions. The first three sets of curves further confirm the predominant effect of temporal resolution, which determines the performance of a given rainfall input, regardless of its spatial resolution, so long as the latter is kept close to the estimated required resolution. The fourth set of curves, corresponding to spatial resolutions of 3000 m and varying temporal resolutions, confirms that the 3000 m resolution largely exceeds the required spatial resolution, thus causing a general drop in performance for all rainfall inputs at this spatial resolution, regardless of their temporal resolution. A similar behaviour is observed in the case of R^2, although for this statistic the 3000 m estimates curves are not grouped together, suggesting that in terms of the pattern of flow hydrographs, as measured by R^2, temporal resolution plays an ever more predominant role, which even overshadows the effect of the coarsest (3000 m) resolution.

5. Summary, conclusions and outlook

The aim of this paper was to quantify the impact of rainfall input resolutions on operational urban drainage modelling outputs and, based upon it, to identify critical resolutions which enable a proper characterisation of urban catchment hydrological response. Using X-band radar-rainfall estimates for nine storm events, initially at 100 m and 1 min resolution, 16 different combinations of spatial and temporal resolutions, up to 3000 m and 10 min, were generated. Coarser spatial resolutions were generated by averaging in space, whereas coarser temporal resolutions were generated by sampling radar images at the desired temporal resolution, thus replicating radar scanning strategies. The resulting rainfall estimates were applied as input to the operational semi-distributed hydrodynamic models of seven urban catchments in North-West Europe, all of which have similar size (between 3 and 8 km^2), but different morphological, hydrological and hydraulic characteristics.

The spatial–temporal characteristics of the storm events, including theoretically required spatial and temporal resolutions given the observed rainfall variability, were derived using geostatistical analysis and storm cell tracking. In addition, the concept of maximum observable singularity, which relies on the framework of Universal Multifractals and allows quantifying higher-order statistical features, was used to quantify the intrinsic variability of rainfall fields at different spatial scales. Hydrodynamic response behaviour was summarised using dimensionless performance statistics and was analysed in the light of drainage area and critical spatial–temporal resolutions computed for each of the storm events.

The main findings and implications of this study are the following:

- Results of the geostatistical analysis and storm cell tracking showed that very fine temporal resolutions, usually below 5 min, are required to properly capture the variability observed in the rainfall data. This requirement is seldom met by rainfall estimates available from national weather radar networks, usually at temporal resolutions of 5 or 10 min. In contrast, the theoretically required spatial resolutions (derived from the geostatistical analysis) appear to be less stringent, with required resolutions ranging between 700 m and 2 km, which are generally met by the radar products provided by national weather services (usually at 1 km resolution). Nonetheless, the multifractal analysis of rainfall fields revealed a break in scaling behaviour between 400 m and 800 m which suggests that rainfall should be measured at sub-kilometric scales, in order to capture structures and extremes which cannot be extrapolated from measurements at coarser resolutions.
- In agreement with previous studies (e.g. Berne et al., 2004; Gires et al., 2012; Lobligeois et al., 2014), the impact of rainfall input resolution on hydraulic outputs was shown to decrease significantly as catchment drainage area increases. For drainage areas of the order of 1 ha errors in peak discharges of up to 250% were observed as a result of rainfall input resolution coarsening, whereas for drainage areas of ~800 ha maximum errors in peak discharge were of the order of 50%.
- Across the entire range of drainage areas under investigation (1–800 ha), the coarsening of temporal resolution of rainfall inputs was shown to have a bigger effect upon hydrodynamic modelling results than the coarsening of spatial resolution. These results are in agreement with the independent

(geostatistical and cell tracking) analysis of the storms and corroborate the need for rainfall input temporal resolutions below 5 min for urban hydrological applications. The strong and dominant effect of temporal resolution coarsening can be partially explained by the way in which coarser temporal resolutions were derived, i.e., by sampling radar images at the desired time step, thus replicating radar scanning strategies. A study focusing on investigating the impact of rainfall temporal resolution coarsening through aggregation (i.e. averaging in time, which resembles the functioning of rain gauges) is currently underway. Initial results indicate that the impact of temporal resolution decreases significantly when coarser temporal resolution estimates are generated through aggregation as opposed to sampling. When aggregation is used, coarsening of spatial and temporal resolutions leads to impacts of comparable magnitudes on estimated runoff, although the latter still has a bigger effect. Similar findings regarding the dominant effect of temporal resolution over spatial resolution have been obtain from other studies, both in rural and urban catchments (Krajewski et al., 1991; Meselhe et al., 2009; Notaro et al., 2013).

- With regards to required rainfall input spatial resolution, this is strongly dependent upon the drainage area of interest. For very small drainage areas, below 1 ha, rainfall input resolutions of ~100 m are required. For drainage areas between 1 ha and ~100 ha, rainfall inputs at a spatial resolution of 500 m appear to be sufficient; for these areas no significant improvement is observed when using finer spatial resolution rainfall estimates and acceptable hydraulic performance is still obtained for rainfall estimates at 1 km/1 min resolution. For drainage areas larger than 100 ha rainfall input spatial resolutions of 1 km appear to be sufficient, leading to high values of performance statistics, as long as the accompanying temporal resolution is fine enough (<5 min). For all drainage areas, rainfall input spatial resolution of 3 km, which may be compared to common distances between rain gauges, appears to be insufficient, leading to very poor hydraulic performance statistics. It can be seen that, in general (except for very small drainage areas) and in agreement with the results of the storm analysis described above, ~1 km resolution rainfall estimates appear to be sufficient for urban hydrological modelling. However, it is important to mention that these results are bound to the storm events under consideration and to the type of models employed in this study; it is, operational semi-distributed, albeit high-resolution models (see subcatchment sizes in Table 2), calibrated using rain gauge records of coarse spatial resolution as input, which may lead to spatially homogeneous model parametrisation (Finnerty et al., 1997). Higher-resolution fully-distributed models, implemented and calibrated using high resolution datasets, are likely to be more sensitive to the spatial resolution of rainfall inputs and may therefore require sub-kilometric resolution rainfall estimates as input (Schertzer et al., 2010; Gires et al., 2014a,b; Pina and Ochoa-Rodriguez, 2014; Ichiba et al., 2015).
- Despite the dominant effect of temporal resolution, the hydraulic results show that there is a strong interaction and dependence between the spatial and temporal resolution of rainfall input estimates. As such, in order to avoid losing relevant information from the rainfall fields, the two resolutions must be in agreement with each other. For example, the hydraulic outputs associated with rainfall inputs at 1000 m/5 min resolution display a better performance than those associated with 100 m/5 min ones. The dependence between spatial and temporal resolutions has been widely discussed (e.g. Kolmogorov, 1962; Schertzer and Lovejoy, 1987; Marsan et al., 1996; Deidda, 2000; Gires et al., 2012), but there is not as yet much evidence in urban hydrology to corroborate this hypothesis. The results of this study do provide evidence to support it.
- The theoretically derived minimum spatial–temporal resolution of rainfall inputs, estimated on the basis of the sole analysis of rainfall images, are consistent with the results of the hydraulic analysis. This validates the proposed approach to characterise storm events and suggests that, in addition to drainage area, a big part of the impact of rainfall input resolution on urban runoff estimates can be explained by the spatial–temporal characteristics of the storm events. The influence of other factors such as catchment and model characteristics was not investigated in detail and remains a topic for future study.

While the present study has several limitations, the results provide useful insights into rainfall input resolution requirements for urban hydrological applications, considering currently available data and models. Evidently, higher spatial and temporal resolution rainfall estimates are desirable. However, resolution comes at a cost and resources are limited. According to the results of this study, rainfall monitoring strategies may consider prioritising improvements in temporal resolution (e.g. modifying radar scanning strategies, using local X-band radars which have higher rotation rates, employing temporal interpolation techniques), while keeping in mind the dependence between temporal and spatial resolutions, as well as the fact that measuring rainfall at higher resolutions can lead to improvements in accuracy. Future research should focus on gathering high resolution rainfall datasets alongside high resolution local urban runoff records and implementation of higher resolution urban drainage models, which enable a better assessment of the added value of high resolution rainfall data and models. Further work is also needed to better understand factors affecting model sensitivity to rainfall input resolution, including storm spatial–temporal characteristics, as well as catchment and model characteristics (e.g. slope, degree of imperviousness, presence of control elements, spatial homogeneity/heterogeneity, amongst others).

Acknowledgements

The authors would like to thank the support of the EU Interreg IVB NWE programme to the RainGain project (www.raingain.eu), which made this international collaboration possible. The first author would like to thank Thames Water and Torbay Council for providing urban drainage models of Cranbrook and Torquay Town Centre, respectively. Thanks are also due to Innovyze for providing InfoWorks licences to researchers at Imperial College London and KU Leuven. Co-authors from KU Leuven would like to acknowledge the support of the Research Foundation–Flanders (FWO) as well as the PLURISK project for the Belgian Science Policy Office. Co-authors of TU Delft would like to thank City of Rotterdam for providing hydrodynamic models of 3 of the city's districts. Co-authors from École des PontsParisTech are grateful to the Chair Hydrology for Resilient Cities of École des PontsParisTech endowed by VEOLIA, for its financial support. Rui Daniel Pina acknowledges the financial support from the Fundação para a Ciência e Tecnologia – Ministério para a Ciência, Tecnologia e Ensino Superior, Portugal [SFRH/BD/88532/2012].

Appendix A. Supplementary material

Supplementary data associated with this article can be found, in the online version, at http://dx.doi.org/10.1016/j.jhydrol.2015.05.035.

References

Arnaud, P., Bouvier, C., Cisneros, L., Dominguez, R., 2002. Influence of rainfall spatial variability on flood prediction. J. Hydrol. 260 (1–4), 216–230.

Aronica, G., Cannarozzo, M., 2000. Studying the hydrological response of urban catchments using a semi-distributed linear non-linear model. J. Hydrol. 238 (1–2), 35–43.
Atkinson, P.M., Aplin, P., 2004. Spatial variation in land cover and choice of spatial resolution for remote sensing. Int. J. Remote Sens. 25 (18), 3687–3702.
Bastin, G., Lorent, B., Duqué, C., Gevers, M., 1984. Optimal estimation of the average areal rainfall and optimal selection of rain gauge locations. Water Resour. Res. 20 (4), 463–470.
Berndtsson, R., Niemczynowicz, J., 1988. Spatial and temporal scales in rainfall analysis — Some aspects and future perspectives. J. Hydrol. 100 (1–3), 293–313.
Berne, A., Delrieu, G., Creutin, J.-D., Obled, C., 2004. Temporal and spatial resolution of rainfall measurements required for urban hydrology. J. Hydrol. 299, 166–179.
Biaou, A., Chauvin, F., Royer, J.F., Schertzer, D., 2005. Analyse multifractale des précipitations dans un scénario GIEC du CNRM. Note de centre GMGEC, CNRM, 101, 45 pp.
Bringi, V.N., Chandrasekar, V., 2001. Polarimetric Doppler Weather Radar Principles and Applications. Cambridge University Press, Cambridge, UK.
Bruni, G., Reinoso, R., van de Giesen, N.C., Clemens, F.H.L.R., ten Veldhuis, J.A.E., 2015. On the sensitivity of urban hydrodynamic modelling to rainfall spatial and temporal resolution. Hydrol. Earth Syst. Sci. 19 (2), 691–709.
Chaubey, I., Haan, C.T., Grunwald, S., Salisbury, J.M., 1999. Uncertainty in the model parameters due to spatial variability of rainfall. J. Hydrol. 220 (1–2), 48–61.
Deidda, R., 2000. Rainfall downscaling in a space-time multifractal framework. Water Resour. Res. 36 (7), 1779–1794.
Douglas, E.M., Barros, A.P., 2003. Probable maximum precipitation estimation using multifractals: application in the Eastern United States. J. Hydrometeorol. 4 (6), 1012–1024.
Einfalt, T., 2005. A hydrologists' guide to radar use in various applications. In: 10th International Conference on Urban Drainage, Copenhagen, Denmark.
Einfalt, T., Arnbjerg-Nielsen, K., Golz, C., Jensen, N.-E., Quirmbachd, M., Vaes, G., Vieux, B., 2004. Towards a roadmap for use of radar rainfall data in urban drainage. J. Hydrol. 299, 186–202.
Emmanuel, I., Andrieu, H., Leblois, E., Flahaut, B., 2012. Temporal and spatial variability of rainfall at the urban hydrological scale. J. Hydrol. 430–431, 162–172.
Fabry, F., Bellon, A., Duncan, M.R., Austin, G.L., 1994. High resolution rainfall measurements by radar for very small basins: the sampling problem reexamined. J. Hydrol. 161, 415–428.
Faurès, J.-M., Goodrich, D.C., Woolhiser, D.A., Sorooshian, S., 1995. Impact of small-scale spatial rainfall variability on runoff modeling. J. Hydrol. 173 (1–4), 309–326.
Fewtrell, T.J., Duncan, A., Sampson, C.C., Neal, J.C., Bates, P.D., 2011. Benchmarking urban flood models of varying complexity and scale using high resolution terrestrial LiDAR data. Phys. Chem. Earth, Parts A/B/C 36 (7–8), 281–291.
Figueras i Ventura, J., 2009. Design of a High Resolution X-Band Doppler Polarimetric Radar. PhD Dissertation, Delft University of Technology, Delft, The Netherlands.
Finnerty, B.D., Smith, M.B., Seo, D.-J., Koren, V., Moglen, G.E., 1997. Space-time scale sensitivity of the Sacramento model to radar-gage precipitation inputs. J. Hydrol. 203 (1–4), 21–38.
Garrigues, S., Allard, D., Baret, F., Weiss, M., 2006. Quantifying spatial heterogeneity at the landscape scale using variogram models. Remote Sens. Environ. 103 (1), 81–96.
Garrigues, S., Allard, D., Baret, F., Morisette, J., 2008. Multivariate quantification of landscape spatial heterogeneity using variogram models. Remote Sens. Environ. 112 (1), 216–230.
Giangola-Murzyn, A., Gires, A., Hoang, C.T., Tchiguirinskaia, I., Schertzer, D., 2012. Multi-Hydro modelling to assess flood resilience across scales, case study in the Paris region. In: 9th International Conference on Urban Drainage Modelling, Belgrade, Serbia.
Gires, A., Tchiguirinskaia, I., Schertzer, D., Lovejoy, S., 2011. Multifractal and spatio-temporal analysis of the rainfall output of the Meso-NH model and radar data. Hydrol. Sci. J. 56 (3), 380–396.
Gires, A., Onof, C., Maksimović, Č., Schertzer, D., Tchiguirinskaia, I., Simoes, N., 2012. Quantifying the impact of small scale unmeasured rainfall variability on urban runoff through multifractal downscaling: a case study. J. Hydrol. 442, 117–128.
Gires, A., Giangola-Murzyn, A., Abbes, J.-B., Tchiguirinskaia, I., Schertzer, D., Lovejoy, S., 2014a. Impacts of small scale rainfall variability in urban areas: a case study with 1D and 1D/2D hydrological models in a multifractal framework. Urban Water J., 1–11
Gires, A., Tchiguirinskaia, I., Schertzer, D., Schellart, A., Berne, A., Lovejoy, S., 2014b. Influence of small scale rainfall variability on standard comparison tools between radar and rain gauge data. Atmos. Res. 138, 125–138.
Gupta, H.V., Kling, H., Yilmaz, K.K., Martinez, G.F., 2009. Decomposition of the mean squared error and NSE performance criteria: implications for improving hydrological modelling. J. Hydrol. 377 (1–2), 80–91.
Horne, M.P., 2003. Short-Term Precipitation Nowcasting for Composite Radar Rainfall Fields. MSc Dissertation, Massachusetts Institute of Technology, Cambridge, USA.
Hubert, P., Tessier, Y., Lovejoy, S., Schertzer, D., Schmitt, F., Ladoy, P., Carbonnel, J.P., Violette, S., Desurosne, I., 1993. Multifractals and extreme rainfall events. Geophys. Res. Lett. 20 (10), 931–934.
Ichiba, A., Gires, A., Tchguirinskaia, I., Bompard, P., Schertzer, D., 2015. High resolution modeling in urban hydrology: comparison between two modeling approaches and their sensitivity to high rainfall variability. In: EGU General Assembly 2015, Vienna, Austria.
Kavetski, D., Kuczera, G., Franks, S.W., 2006. Bayesian analysis of input uncertainty in hydrological modeling: 1. Theory. Water Resour. Res. 42 (3), W03407.
Kolmogorov, A.N., 1962. A refinement of previous hypotheses concerning the local structure of turbulence in a viscous incompressible fluid at high Reynolds number. J. Fluid Mech. 13 (01), 82–85.
Krajewski, W.F., Lakshmi, V., Georgakakos, K.P., Jain, S.C., 1991. A Monte Carlo Study of rainfall sampling effect on a distributed catchment model. Water Resour. Res. 27 (1), 119–128.
Krause, P., Boyle, D.P., Base, F., 2005. Comparison of different efficiency criteria for hydrological model assessment. Adv. Geosci. 5, 89–97.
Lantuéjoul, C., 1991. Ergodicity and integral range. J. Microsc. 161 (3), 387–403.
Lantuéjoul, C., 2002. Geostatistical Simulation – Models and Algorithms. Springer, Berlin, Germany.
Laroche, S., Zawadzki, I., 1995. Retrievals of horizontal winds from single-doppler clear-air data by methods of cross correlation and variational analysis. J. Atmos. Oceanic Technol. 12 (4), 721–738.
Leijnse, H., Uijlenhoet, R., van de Beek, C.Z., Overeem, A., Otto, T., Unal, C.M.H., Dufournet, Y., Russchenberg, H.W.J., Figueras i Ventura, J., Klein Baltink, H., Holleman, I., 2010. Precipitation measurement at CESAR, the Netherlands. J. Hydrometeorol. 11 (6), 1322–1329.
Li, P.W., Lai, E.S.T., 2004. Short-range quantitative precipitation forecasting in Hong Kong. J. Hydrol. 288 (1–2), 189–209.
Lobligeois, F., Andréassian, V., Perrin, C., Tabary, P., Loumagne, C., 2014. When does higher spatial resolution rainfall information improve streamflow simulation? An evaluation using 3620 flood events. Hydrol. Earth Syst. Sci. 18 (2), 575–594.
Marsan, D., Schertzer, D., Lovejoy, S., 1996. Causal space-time multifractal processes: predictability and forecasting of rain fields. J. Geophys. Res.: Atmos. 101 (D21), 26333–26346.
Meselhe, E., Habib, E., Oche, O., Gautam, S., 2009. Sensitivity of conceptual and physically based hydrologic models to temporal and spatial rainfall sampling. J. Hydrol. Eng. 14 (7), 711–720.
Murphy, A.H., 1988. Skill scores based on the mean square error and their relationships to the correlation coefficient. Mon. Weather Rev. 116 (12), 2417–2424.
Notaro, V., Fontanazza, C.M., Freni, G., Puleo, V., 2013. Impact of rainfall data resolution in time and space on the urban flooding evaluation. Water Sci. Technol. 68 (9), 1984–1993.
Obled, C., Wendling, J., Beven, K., 1994. The sensitivity of hydrological models to spatial rainfall patterns: an evaluation using observed data. J. Hydrol. 159 (1–4), 305–333.
Ogden, F.L., Julien, P.Y., 1994. Runoff model sensitivity to radar rainfall resolution. J. Hydrol. 158 (1–2), 1–18.
Otto, T., Russchenberg, H.W.J., 2011. Estimation of specific differential phase and differential backscatter phase from polarimetric weather radar measurements of rain. Geosci. Remote Sens. Lett., IEEE 8 (5), 988–992.
Otto, T., Russchenberg, H.W.J., 2012. Rainfall rate retrieval with IDRA, the polarimetric X-band radar at Cabauw, NL. In: 7th European Conference on Radar Meteorology and Hydrology, Toulouse, France.
Pina, R., Ochoa-Rodriguez, S., 2014. Fully-distributed vs. Semi-distributed urban drainage models. In: RainGain International Workshop on Urban Pluvial Flood Models, Exeter, UK.
Pina, R., Ochoa-Rodríguez, S., Simoes, N., Mijic, A., Sa Marques, A., Maksimovic, Č., 2014. Semi-distributed or fully distributed rainfall-runoff models for urban pluvial flood modelling? In: 13th International Conference on Urban Drainage, Sarawak, Malaysia.
Rinehart, R.E., Garvey, E.T., 1978. Three-dimensional storm motion detection by conventional weather radar. Nature 273 (5660), 287–289.
Royer, J.-F., Biaou, A., Chauvin, F., Schertzer, D., Lovejoy, S., 2008. Multifractal analysis of the evolution of simulated precipitation over France in a climate scenario. C.R. Geosci. 340 (7), 431–440.
Scarchilli, G., Gorgucci, E., Chandrasekar, V., 1996. Self-consistency of polarization diversity measurements of rainfall. IEEE Trans. Geosci. Remote Sens. 34 (1), 22–26.
Schellart, A.N.A., Shepherd, W.J., Saul, A.J., 2012. Influence of rainfall estimation error and spatial variability on sewer flow prediction at a small urban scale. Adv. Water Resour. 45, 65–75.
Schertzer, D., Lovejoy, S., 1987. Physical modeling and analysis of rain and clouds by anisotropic scaling multiplicative processes. J. Geophys. Res. 92 (D8), 9693–9714.
Schertzer, D., Lovejoy, S., 2011. Multifractals, generalized scale invariance and complexity in geophysics. Int. J. Bifurcation Chaos 21 (12), 3417–3456.
Schertzer, D., Tchiguirinskaia, I., Lovejoy, S., Hubert, P., 2010. No monsters, no miracles: in nonlinear sciences hydrology is not an outlier! Hydrol. Sci. J. 55 (6), 965–979.
Schilling, W., 1991. Rainfall data for urban hydrology: what do we need? Atmos. Res. 27, 5–21.
Segond, M.L., Neokleous, N., Makropoulos, C., Onof, C., Maksimović, Č., 2007. Simulation and spatio-temporal disaggregation of multi-site rainfall data for urban drainage applications. Hydrol. Sci. J. – J. Des Sci. Hydrol. 52 (5), 917–935.
Shah, S.M.S., O'Connell, P.E., Hosking, J.R.M., 1996. Modelling the effects of spatial variability in rainfall on catchment response. 2. Experiments with distributed and lumped models. J. Hydrol. 175 (1–4), 89–111.
Shannon, C.E., 1948. A mathematical theory of communication. Bell Syst. Tech. J. 27 (3), 379–423.

Singh, V.P., 1997. Effect of spatial and temporal variability in rainfall and watershed characteristics on stream flow hydrograph. Hydrol. Process. 11 (12), 1649–1669.
Smith, M.B., Koren, V.I., Zhang, Z., Reed, S.M., Pan, J.-J., Moreda, F., 2004. Runoff response to spatial variability in precipitation: an analysis of observed data. J. Hydrol. 298 (1–4), 267–286.
Syed, K.H., Goodrich, D.C., Myers, D.E., Sorooshian, S., 2003. Spatial characteristics of thunderstorm rainfall fields and their relation to runoff. J. Hydrol. 271 (1–4), 1–21.
Tabios, G.Q., Salas, J.D., 1985. A comparative analysis of techniques for spatial interpolation of precipitation. JAWRA J. Am. Water Resour. Assoc. 21 (3), 365–380.
Tetzlaff, D., Uhlenbrook, S., 2005. Significance of spatial variability in precipitation for process-oriented modelling: results from two nested catchments using radar and ground station data. Hydrol. Earth Syst. Sci. 9, 29–41.
Tuttle, J.D., Foote, G.B., 1990. Determination of the boundary layer airflow from a single doppler radar. J. Atmos. Oceanic Technol. 7 (2), 218–232.
Unal, C., 2009. Spectral polarimetric radar clutter suppression to enhance atmospheric echoes. J. Atmos. Oceanic Technol. 26 (9), 1781–1797.
Vieux, B.E., Imgarten, J.M., 2012. On the scale-dependent propagation of hydrologic uncertainty using high-resolution X-band radar rainfall estimates. Atmos. Res. 103, 96–105.
Wang, L.-P., Onof, C., Ochoa-Rodríguez, S., Simoes, N.E., Maksimović, Č., 2012. On the propagation of rainfall bias and spatial variability through urban pluvial flood modelling. In: 9th International Workshop on Precipitation in Urban Areas: Urban challenges in rainfall analysis, Saint Moritz, Switzerland.
Wang, L.-P., Ochoa-Rodríguez, S., Simoes, N., Onof, C., Maksimović, Č., 2013. Radar-raingauge data combination techniques: a revision and analysis of their suitability for urban hydrology. Water Sci. Technol. 68 (4), 737–747.
Wang, L.P., Ochoa-Rodríguez, S., Onof, C., Willems, P., 2015. Singularity-sensitive gauge-based radar rainfall adjustment methods for urban hydrological applications. Hydrol. Earth Syst. Sci. Discuss. 12 (2), 1855–1900.
WAPUG, 2002. Code of Practice For The Hydraulic Modelling of Sewer Systems, Wastewater Planning Users Group.